

A prototype stochastic model for salmon management.

Project SF0274 September 2008 milestone (2)

WILLIAM S.C. GURNEY^{*1,2} AND PHILIP BACON³

¹*Strathclyde Fisheries Institute, University of Strathclyde, GLASGOW, Scotland*

²*F.R.S. Marine Laboratory, ABERDEEN, Scotland.*

³*F.R.S. Freshwater Laboratory, PITLOCHRY, Scotland.*

*Corresponding author

Executive summary

We have studied stock-recruitment data from a number of Scottish locations including the Girnock Burn and the North Esk, and conclude that:

- The shape of the mean stock-recruitment relation at low stock levels plays a critical role in determining the degree to which demographic and environmental variability influence population persistence.
- This low-stock shape is systematically poorly defined by empirical data, implying that mechanistic descriptions of the underlying mechanisms form the only plausible route to reducing uncertainty and consequent policy risks.

We have studied a number of simple stochastic models of stock-recruitment controlled population dynamics, from which we infer that:

- The serial correlation of population fluctuations driven by recruitment and survival variability is critically related to the age range of returning spawners. If all individuals return at the same age the population divides into a group of unconnected ‘lineages’ and there is no correlation between spawning populations in sequential years. This has clear implications for management actions predicated on observations the previous year.
- Generational correlations can be positive, negative or insignificant according to the shape of the stock-recruitment relation and the position of the mean population with respect to the S-R maximum. Populations with mean stocks well below the S-R maximum tend to be vulnerable and it may be possible to identify such vulnerability from the ACF of an observed time-series.
- Short-term correlation in spawning stock fluctuations is frequently weak, in which case simplistic conservation limit (CL) driven management policies (for example defining the allowable catch this year equal to the excess of last year’s spawning stock over a fixed limit) will produce seriously deleterious effects even when applied to a statistically uniform and well characterised population.
- Where spawners return uniformly over three years, simplistic CL driven exploitation (catch based on last year’s excess) systematically underexploits good years and overexploits bad ones, thereby inducing short period population fluctuations of considerably greater intensity than those implied by natural variability in recruitment and survival.
- Where spawners return predominantly at a single age, ‘pseudo-lineages’ are regularly driven to extinction and only rekindled by leakage from their cousins. As a result both the mean spawning stock and the long-run average catch are far below those which would be obtained by constant effort exploitation.

We believe that with the addition of separate representations of male and females and of grilse, MSW salmon and the genetic linkage between them, year-on-year stochastic models suitable for informing operational management can be constructed. We have implemented one such model as a proof of concept, and showed that:

- The relativity of grilse and MSW salmon numbers, and the changes observed in this relativity over four decades in the Girnock Burn can be satisfactorily replicated.
- The serial correlation behaviour of the more complex model is very close to that observed in its strategic precursors, so our earlier conclusions concerning the inadvisability of basing short-term management actions on immediate prior year excess over CL appear robust.
- The computational efficiency of the model is such that stochastic projection, in which the full probability distribution (including the probability of extinction) for future populations is calculated, is an achievable aim.

1. Introduction

This report begins by discussing the estimation of the relationship between spawning stock and recruitment in salmon population data. Although such relationships are without exception highly stochastic they are often characterised by a smooth curve which formally represents the mean recruitment outcome at each spawner abundance. We discuss the estimation of mean stock recruitment curves and consider the identification of site to site variations from datasets from the Girnock Burn, the N. Esk (both in Scotland) and the River Bush (N. Ireland).

We note that typical data defines the form of the mean stock-recruitment relation poorly and we discuss the implications of this uncertainty for identification of the deterministic dynamics of a given stock.

We next consider stochastic stock-recruitment relations and investigate their influence in driving generation to generation and year to year stock fluctuations. We develop a computationally efficient stochastic population model as a strategic representation of a catchment sub-population. We use this model to consider the relation between year to year correlation in population fluctuations and the temporal pattern of return to spawn. Finally we investigate the effects of simple conservation limit driven management policies (which base the allowable catch in a given year on the amount by which the previous year's spawning stock exceeds a fixed limit) on the stability, persistence and yield of an exploited salmon population.

Not unexpectedly, we find that the serial correlation between spawning stock in successive years is critical in determining the efficacy of such a policy. In general, the smaller the dispersion in river age at smolting and the larger the stochastic variability in survival, the smaller the serial correlation between years. Realistic parameters for the Girnock burn (with returns occurring in almost equal numbers at absolute ages over a three year span) imply that such a policy systematically tends to over exploit poor years and underexploit good ones, leading to reduced medium term average yields relative to constant effort exploitation, while also inducing more intense fluctuations than those which would occur under a constant effort regime.

In view of the importance of survival variability in determining serial correlation, we next investigated the robustness of these conclusions against an extension of the model to incorporate independent representation of males and females and of grilse and MSW salmon. To facilitate this investigation we defined a generic framework for modelling stock recruitment driven salmon populations in which sea-age at return is heritable. Using this framework we implemented a model of an upland salmon sub-catchment population in which grilse/MSW return is determined at a single genetic locus.

This model demonstrated that the conclusions from our earlier investigation of strategic salmon population models are robust. However, the fidelity with which our prototype model reproduced the qualitative sequence of events observed in the Girnock Burn between 1967 and 2003 has led us to believe that this model framework can form the basis upon which operational models for whole catchment salmon population models can be constructed.

2. Observed stock-recruitment curves

2.1. Sigmoidal Ricker stock-recruitment

Stock-recruitment relations are very often fitted using the standard Ricker form

$$R_t = R_{max} \left[\frac{S_t}{S_{max}} \right] \exp \left[1 - \frac{S_t}{S_{max}} \right] \quad (1)$$

where R_{max} is the maximum possible population output of recruits and S_{max} is the number of reproductively active adults (spawning stock) who produce this output. In this investigation we use a modified form of this relation, which allows the curve to have a sigmoidal form, namely

$$R_t = R_{max} \left[\frac{S_t}{S_{max}} \right]^k \exp \left[k \left(1 - \frac{S_t}{S_{max}} \right) \right] \quad (2)$$

where R_{max} and S_{max} retain their original interpretation and k is the sigmoidality parameter. We shall hereafter refer to this functional form as the Sigmoidal Ricker (SR) stock recruitment curve.

When $k \leq 1$ the slope of the SR curve decreases monotonically as S_t rises from zero, with the slope at zero being infinite for all $k < 1$ and finite for $k = 1$. When $k > 1$ the slope at the origin is zero and initially increases with S_t (see Fig. 1b).

If the species concerned is semelparous, the proportion of recruits who survive to spawn is P , and all individuals who spawn do so after g years, then the population dynamics are described by

$$S_{t+g} = PR_{max} \left[\frac{S_t}{S_{max}} \right]^k \exp \left[k \left(1 - \frac{S_t}{S_{max}} \right) \right] \quad (3)$$

Equilibrium in this system clearly requires each spawner to produce exactly one spawning adult in the next generation, that is the net reproduction per individual spawner (r) must be unity, i.e.

$$r_t \equiv \left[\frac{PR_{max}}{S_{max}} \right] \left[\frac{S_t}{S_{max}} \right]^{k-1} \exp \left[k \left(1 - \frac{S_t}{S_{max}} \right) \right] = 1. \quad (4)$$

If all a cohort's members do not spawn simultaneously, the population's transient dynamics are no longer described by equation (3), but the requirement for equilibrium is still equation (4).

Examination of Fig. 1a lets us identify the number and stability of stationary solutions to equation (3). If $k < 1$ then there is always exactly one solution with $S^* > 0$ which is guaranteed to be an attractor. If $k = 1$, then there is a single attracting stationary solution provided that $r(0)$ is greater than 1, that is

$$\frac{PR_{max}e^1}{S_{max}} > 1 \quad \Leftrightarrow \quad P > P_c^R \equiv \frac{S_{max}e^{-1}}{R_{max}}, \quad (5)$$

and no non-zero stationary solution otherwise. If $k > 1$ then there are two non-zero solutions or none. If the maximum value of r is smaller than unity then there is a single attracting solution at the origin ($S^* = 0$). If it is larger than unity, this solution is joined by two more, the lower one being a repeller and the upper an attractor. Thus, for $k > 1$

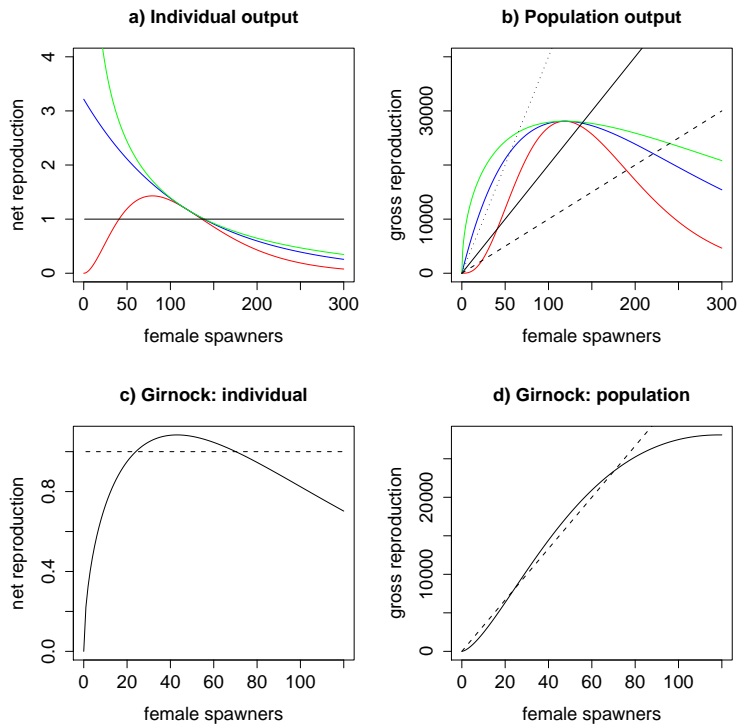


Figure 1: The Sigmoidal Ricker stock recruitment curve. *a)* and *b)* illustrate the behaviour of this relation for $k = 0.5$ (green), $k = 1$ (blue) and $k = 3$ (red). *a)* shows the implied net individual reproductive output (equation 4) if the survival to spawn $P = 0.005$ compared to the equilibrium requirement (black line), *b)* shows the gross population reproductive output (equation 2) compared to that needed for equilibrium when $P = 0.005$ (solid line), $P = 0.01$ (dashed line) and $P = 0.0025$ (dotted). *c)* and *d)* show net individual and gross population reproduction for the Girnock (spawner-fry) best fits ($R_{max} = 28095$, $S_{max} = 118.7$, $k = 1.569$) compared to the equilibrium requirement if $P = 0.003$, implying a steady state population of about 70 females.

the system has one non-zero attracting solution, with a basin of attraction bounded below by the second interior steady state. A few lines of elementary algebra suffice to show that the requirement for the existence of such a solution is

$$P > P_c^M \equiv \frac{S_{max}e^{-1}}{R_{max}} \cdot \left[\frac{k}{k-1} \right]^{k-1}. \quad (6)$$

2.2. Fitting the SR stock recruitment curve to data.

To investigate the shape of observed stock-recruitment curves we have fitted the Sigmoidal Ricker (and some alternative forms) to a number of datasets. In each case we determined the best fit to the data using the Nelder-Meade non-linear optimisation algorithm implemented in the R routine ‘optim’. The best fit curves implied by this process, together with the observations are shown in Fig. 2.

Examination of the standardised residuals yielded by the fitting process (see Appendix A) suggests that their standard deviation at any given spawner number is proportional to the fitted mean. To determine confidence limits for the fitted curves we generated a

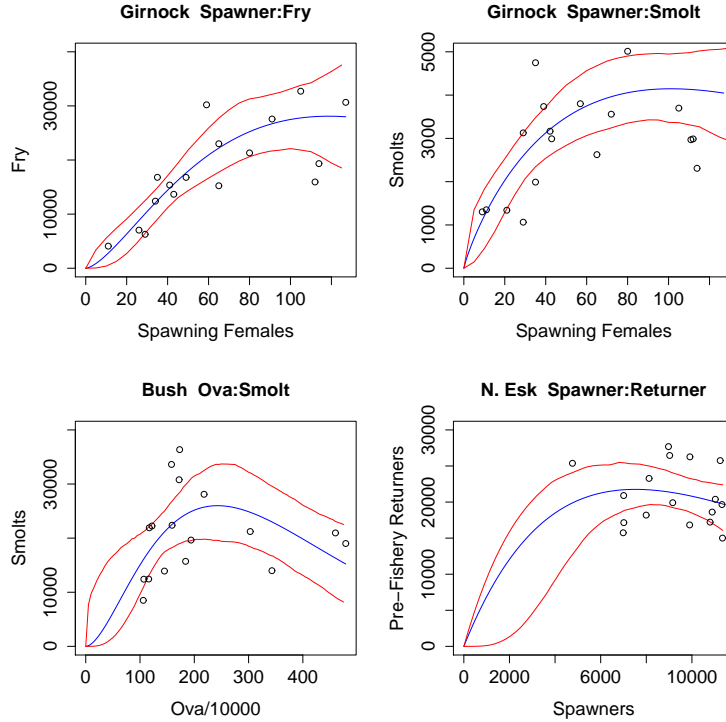


Figure 2: Sigmoidal Ricker curves fitted to data from the Girnock Burn and the rivers Bush and N. Esk. In all cases the points show observations, the blue line shows the best fit and the red lines show 95% confidence limits. a) shows a fit to the fry abundance in the Girnock determined from electrofishing data for the years 1968-78, 1981-89 and 1999. Best fit parameters are $R_{max} = 28096$, $S_{max} = 118.7$, $k = 1.569$. b) shows a fit to Girnock smolt trap data for the years 1966-76, 1981-89, 1992-99. Best fit parameters are $R_{max} = 4145.9$, $S_{max} = 101.17$, $k = 0.87247$. c) shows data on ova input and smolt output for the river Bush for 1973-89 (<http://ram.biology.dal.ca/ftp/pub/sr/ASALBUS2.dat>). Best fit parameters against $ova \times 10^{-5}$ are $R_{max} = 25997$, $S_{max} = 242.9$, $k = 1.828$. d) shows data on spawners and pre-fishery adult returners from the N. Esk, which were fitted with the constraint $k \geq 1$. Best fit parameters are $R_{max} = 21759$, $S_{max} = 7522$, $k = 1.000$.

thousand (statistically equivalent) simulated data sets with points at the same spawner numbers as the observed dataset. Output at those spawner numbers was drawn from a normal distribution with mean equal to the best fit and standard deviation equal to the product of that mean with the overall standard deviation of the standardised residuals. We fitted each simulated dataset in the same way as the observations and then scanned the envelope of predicted curves to find the 2.5% and 97.5% percentiles for each input value. The resulting confidence limits are shown in Fig. 2. The full parameter distributions and samples of the simulated data are shown in Appendix A.

We note from Appendix A.3 that the R^2 for the Bush fit given here is 0.227 which contrasts rather unfavourably with the value of 0.422 claimed by Crozier and Kennedy when fitting the same data with a standard Ricker curve. We have refit this data with a standard (two parameter) Ricker curve and find $R^2 = 0.183$. Perhaps not coincidentally $\sqrt{0.183} = 0.427$ which is very close to Crozier and Kennedy's result if they erroneously identified R as R^2 .

We also note that the fit to the N. Esk data (which might arguably be more appropri-

ately fitted by a horizontal straight line – see Appendix A.8) was constrained to have the sigmoidality parameter $k \geq 1$, in contrast to the other three fits in which the constraint was $k > 0$. Alternative fits to this data with weaker constraints showed that the best fit value of k was always close to the constraint value, leading to best fit lines which are essentially horizontal down to very low values of spawner numbers.

2.3. Steady states, noise and persistence

To aid understanding of the way steady states vary with model parameters, we restate equation (3) as a requirement that any equilibrium state S^* must be a solution of

$$\frac{1}{P}S^* = R_{max} \left[\frac{S^*}{S_{max}} \right]^k \exp \left[k \left(1 - \frac{S^*}{S_{max}} \right) \right] \quad (7)$$

The R.H.S. of this relation is just the stock recruitment curve, while the L.H.S is a straight line through the origin with slope $1/P$. An equilibrium occurs wherever these two are equal, that is where the ‘replacement line’ intersects the stock recruitment curve.

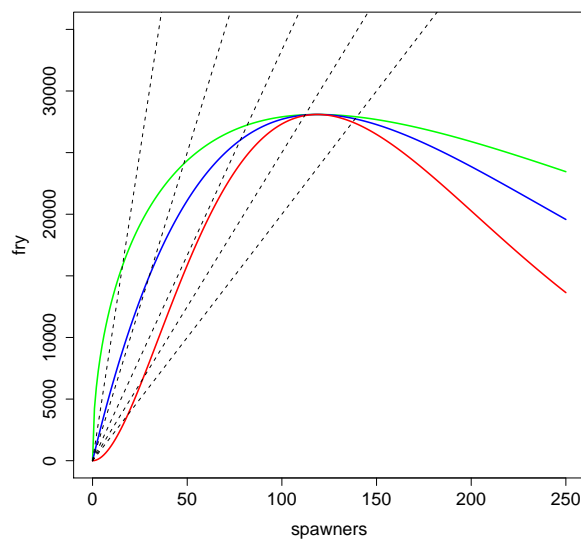


Figure 3: Stock-Recruitment Curves and Steady States. The three solid curves show possible stock-recruitment curve shapes given by equation (2) with $k=0.5$ (green), 1 (blue) and 2 (red). The dotted lines show the renewal condition for five values of P ranging from 0.005 (extreme right) to 0.001 (extreme left).

We illustrate this for three characteristic stock recruitment curve shapes in Fig. 3. When the survival to spawn (P) is ‘large’ then all three curve shapes predict an attracting steady state. However, as P decreases the behaviour of the three curve types diverges. Only for the (rather implausible) case of $k < 1$ does the steady state exist regardless of the value of P . When $k = 1$ (that is for the standard Ricker) the interior ($S^* > 0$) steady state exists only so long as the slope of the replacement line ($1/P$) is less than that of the stock-recruitment

relation at the origin. The requirement that this should be so is that $P > P_c^R$ given by inequality (5). When this inequality is reversed the population experiences ‘deterministic extinction’.

When $k > 1$ the behaviour is even more complex. Here there are two positive steady states, the upper one being the attractor and the lower being a threshold below which the population crashes to zero. When P is large, the threshold steady state is close to the origin and will have no practical effect. However as P decreases (the slope of the replacement line increases) the upper and lower steady states converge and eventually meet when $P = P_c^M$ (equation 6). For $P < P_c^M$ the only steady state is the origin, so the population crashes (deterministically) to extinction.

The foregoing discussion shows that sigmoidality of the stock-recruitment relation (the value of k) has considerable influence on the survival to spawn at which the population experiences deterministic extinction. However, its importance is greatly increased when we take recruitment and survival variability into account. In Fig. 4 we show a series of

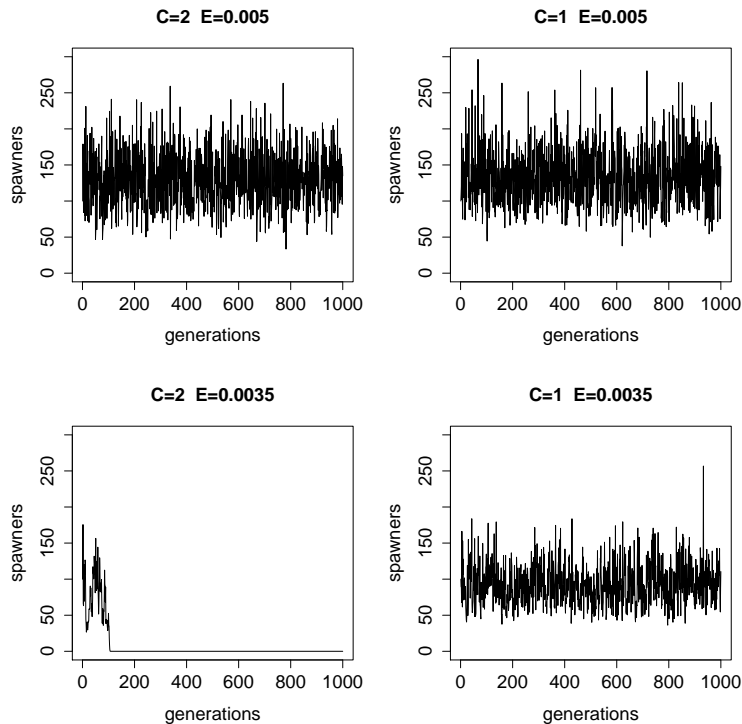


Figure 4: Stochastic Simulations with recruitment negative binomially distributed ($\theta = 15 \Rightarrow c.v. \approx 0.25$) around the mean shown in Fig. 3 for $k = 2$ (left-hand frames) and $k = 1$ (right-hand frames) and P normally distributed around 0.005 (upper frames) or 0.0035 (lower frames) with $CV=0.1$. The mean time to extinction for the case in the lower left frame is 50.9 generations.

simulations in which we assume that for any given value of spawning stock the recruitment is negatively binomially distributed around the mean recruitment appropriate to that stock (see Fig. 3) with a shape factor $\theta = 15$, which approximates to a c.v. of around 25% for spawning stocks from 10-100 females. To add an additional element of realism we also

assume that the survival to spawn P is normally distributed around its designated mean value with a c.v. of 10%.

In the upper frames of the figure we show simulations with mean survival to spawn well above the critical value for $k = 2$ ($P_c^M = 0.0031$). In this case the lower (threshold) and upper steady states for $k = 2$ are about 20 and 100 females respectively and the behaviour of the model with $k = 2$ is remarkable similar to that with $k = 1$. However, with a mean survival to spawn of 0.0035 (which is still comfortably above the critical level for deterministic extinction when $k = 2$), the lower and upper steady states are around 30 and 70 respectively and the stochastic population trajectory goes quite rapidly to extinction – the mean time to extinction for these parameters being 50.9 generations. By contrast the model with $k = 1$ (and hence critical survival to spawn $P_c^R = 0.0015$) shows continued statistically stable variability around the expected mean population.

These simulations show that the details of the low-stock shape of the stock recruitment relation can have a very significant effect on the possibility of both stochastic and deterministic extinction. This leads to a rather serious difficulty in setting conservation limits. Few populations will explore the very low stock region of the stock-recruitment curve very frequently. Indeed, if the curve is S-shaped, any stock which does so is bound for almost certain extinction in the absence of remedial measures.

Hence, to add to the general chronic lack of stock recruitment data, we can add a further impediment, that even good (long-term) data for spatially restricted regions such as the Girnock are unlikely to define the low-stock behaviour well. Shorter term datasets for spatially extended regions are likely to yield no useful information at all on this critical region of the stock recruitment curve.

Prudent discussion of whether a stock is or is not endangered must take appropriate account of the uncertainty in the low-stock shape of the stock-recruitment curve, and acknowledge the possibility that it may be curved in such a way as to enhance the noise sensitivity of the population and hence its probability of becoming extinct. The only practical way to meet this requirement is to develop sufficient understanding of the mechanisms which determine the stock-recruitment relationship, so that a fit to the high-stock region of the curve can be confidently extrapolated to the low-stock region. To fail to do so, for example by simply assuming a standard Ricker curve through a highly dispersed set of data is likely to yield very poor management advice.

2.4. A strategic model of population fluctuations in a single deme

The strategic population model defined by equation (3) assumes that offspring of individuals who reproduce in year y themselves reproduce in year $y + g$. The implication of this assumption is that the population divides into g unconnected ‘lineages’ whose fluctuations are completely uncorrelated (see Fig. 5). To develop a better understanding of the fluctuations in real populations we need to represent the fact that even individuals who return after a fixed number of sea winters may have spent different lengths of time in the river and thus have spent different amounts of time since they were ova.

To facilitate development of a year-by-year (as opposed to generation by generation) model we first define total age a as the age of a returner *since it was spawned*. We now use S_y to represent the number of spawners in year y and $R_y(S_y)$ to denote the number of individuals recruited to the population as a result of the spawning activity in that

year. If the proportion of these recruits who survive to spawn (at any age) is P_y and the proportion of those survivors who spawn at total age a is $Q_y(a)$ then the total spawning population in year Y is given by

$$S_Y = \sum_{y=Y-1}^{Y-a_m} Q_y(Y-y)P_yR(S_y) \quad (8)$$

where a_m is the maximum age at which any individual ever returns to spawn.

In the deterministic variant of this model the stock recruitment function R_y is a deterministic function \hat{R} , the spawning survival P_y is a constant \hat{P} and the return fraction Q_y is a deterministic function \hat{Q} . In this case the steady state S^* is a solution of

$$S^* = \sum_{y=Y-1}^{Y-a_m} \hat{Q}(Y-y)\hat{P}\hat{R}(S^*) = \hat{P}\hat{R}(S^*) \sum_{y=Y-1}^{Y-a_m} \hat{Q}(Y-y) = \hat{P}\hat{R}(S^*), \quad (9)$$

thus demonstrating that the equilibrium requirement is equation (4).

A plausible stochastic variant of the model continues to regard the return fraction $Q(a)$ as a deterministic function, but regards the stock recruitment and survival to spawn as random variables. Following our earlier practice, we define the survival to spawn P as a normally distributed random variable with mean \hat{P} , and the stock recruitment as a negative binomially distributed random variable with (constant) shape factor θ and mean related to the spawning stock by equation (2). This model is extremely simple to simulate (R code to do so is given in Appendix B.1).

Fig. 5 shows results of two simulations. Both depict a population of individuals who return after two sea-winters to spawn with a mean output given by a standard Ricker stock recruitment relation with $S_{max} = 120$. The parameters are chosen so as to put the deterministic steady state ($S^* = 168.5$) well above the maximum of the stock-recruitment curve. One simulation assumes that all individuals smolt after 3 years in the river (that is at $a = 6$) while the other assumes that 50% of returners spawn at $a = 5$ while the remainder spawn at $a = 6$.

Both simulations show statistically stationary fluctuations around means (162 for the 6 year return, 165.4 for the 5 and 6 year returns) which are close to the deterministic stationary state. As we might expect the amplitude of the fluctuations is smaller in the case where returns are spread over two years (six year returns $\Rightarrow CV_S = 35\%$, five and six year returns $\Rightarrow CV_S = 25\%$). Again as we might expect, the ACF's show that if the returners from a given years spawning all arrive in a single year, the population in effect consists of a group of independent (and thus uncorrelated) sub-units, whereas if returners are spread over more than one year, there is significant year to year correlation in fluctuations.

A final point of interest from the ACF's shown in Fig. 5 is that the correlation between generations is negative. We hypothesise that this occurs because the mean spawner population in these simulations is well above the maximum of the S-R curve. In this case a larger than average spawner population will produce a smaller than average recruitment and vice-versa. This suggests that if the mean spawner population is below the maximum of the stock-recruitment curve we should expect a positive generational correlation.

This hypothesis is confirmed by the simulations shown in Fig. 6, which also demonstrate

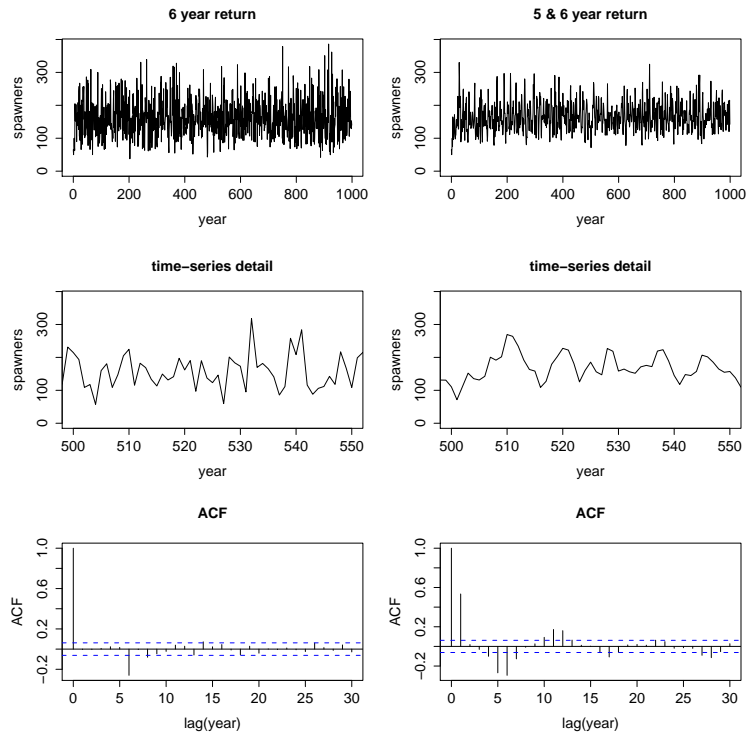


Figure 5: Year by year stochastic simulations of the single deme model. Left hand frames show a 1000 year simulated time series (top), a 50 year time-series segment (middle), and the autocorrelation function (bottom) for a run with all spawners returning at total age $a = 6$ – corresponding to a two sea-winter fish which spends three years in the river. The right hand frames show an identical simulation except that the returning spawners arrive in equal numbers at ages 5 and 6. Common model parameters are: $R_{max} = 3 \times 10^4$, $S_{max} = 120$, $k = 1$, $\theta = 10$, $\hat{P} = 0.006$, $CV_P = 0.1$.

that if the mean is close to the maximum of the S-R curve, the generational correlation disappears. This experiment also demonstrates that the number of year-classes which show positive year to year correlation is determined by the width of the return probability distribution $Q(a)$.

2.5. Managing a single deme - conservation limits

In this section we use the single deme model developed above to explore the implications of conservation limits in salmon management. We base our investigation on the Girnock spawner-smolt data which we fit with a broken-stick stock recruitment curve (see Appendix A.6) to mimic current conservation practice. We postulate that the spawning population in year y is the difference between the numbers returning to the coastal region and the catch in year y which we denote by C_y . We examine two models. In the first model variant, post return exploitation is supposed to remove a constant fraction of the returners (which we call the river exploitation fraction and denote by ρ). In the second, the number of individuals removed after return to the coastal region is equal to the difference between a conservation limit and the previous year's spawning stock, or to the current spawning stock, whichever is smaller.

We explore the effects of these models of exploitation on two systems. In one, the

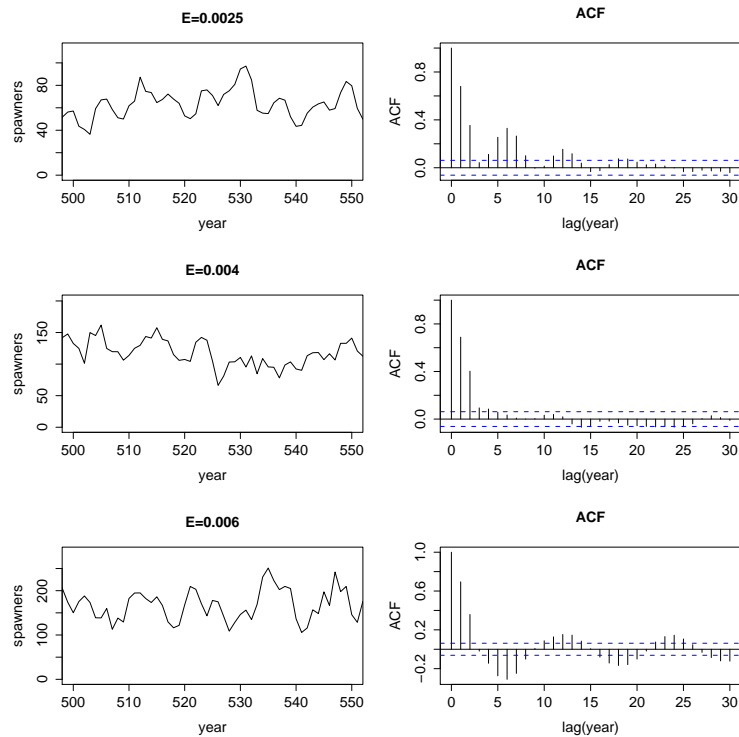


Figure 6: The effect of changing mean on the ACF of population fluctuations. This figure shows a series of simulations with $R_{max} = 3 \times 10^4$, $S_{max} = 120$, $k = 1$, $\theta = 10$, $CV_P = 0.1$ and spawner return occurring with equal probability at $a = 5, 6$ and 7 . The top frames show a run with $\hat{P} = 0.0025$ implying $\hat{S} = 64.4$. The middle frames show a run with $\hat{P} = 0.004$ implying $\hat{S} = 118.8$. The bottom frames show a run with $\hat{P} = 0.006$ implying $\hat{S} = 166.9$.

returning spawners from a given hatch class arrive with equal probability at ages 5, 6 and 7, thus ensuring that the population fluctuations have strong serial correlation. In the other we assume that 80% of the returners are aged 6, with the remaining 20% divided equally between ages 5 and 7. This implies population fluctuations with weak serial correlation.

The results of our simulations are shown in Fig. 7. We have set the combination of river exploitation (50%) and the sea-survival (4%) so as to give a deterministic steady state of 80 females. Constant effort river-exploitation gives a long-term mean population of around 79 females and an almost exactly equal long-term mean yearly catch in both the strong and weak serial correlation cases.

To apply the conservation limit policy we set the CL at 50 individuals, although we note that this experiment is quite favourable to this policy. Appendix A.6 shows the confidence limits on S_{max} to be such that we should expect to get its value wrong by as much as 20% even if we have correctly identified the functional form of the stock-recruitment relation. If we have misidentified the shape of the stock-recruitment relation then our likely error will be much larger.

Despite strong structural similarities between the strong and weak serial correlation cases, the results of applying CL determined exploitation are much more severe in the weak serial correlation case. In both cases we see that the tendency of the CL policy to allow high exploitation after a strong returning year class and close down exploitation

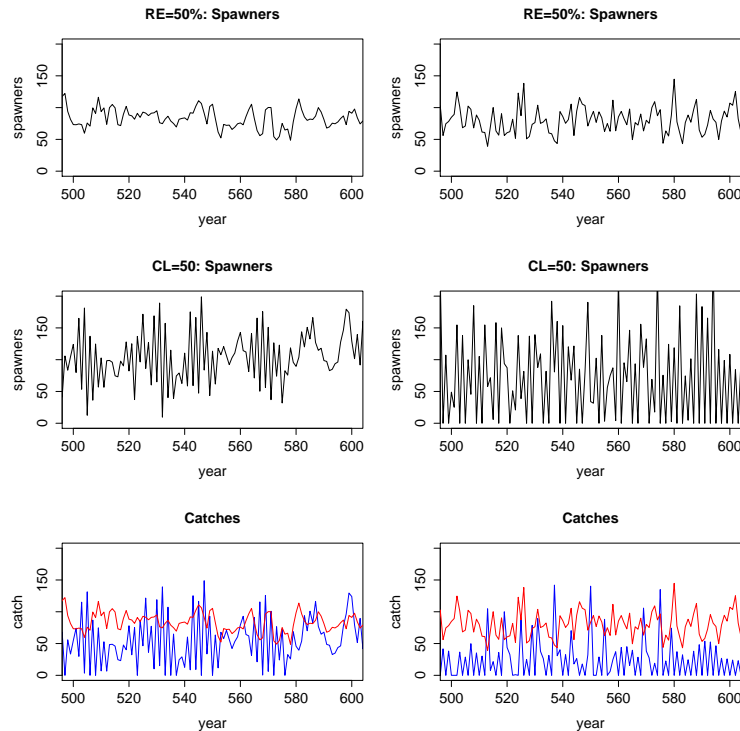


Figure 7: The effects of conservation limited exploitation. This figure shows a series of simulations driven by a broken-stick stock recruitment curve with $R_{max} = 4 \times 10^3$, $S_{max} = 50$, $\theta = 10$, mean sea-survival $\hat{P}=0.04$ and $CV_P = 0.1$. In the left-hand column spawner return occurs with equal probability at $a = 5, 6$ and 7 . In the right-hand column 80% of return is at $a = 6$ with 10% in each of the preceding and succeeding years. The top frames show a run with river exploitation $\rho = 0.5$. The middle frames show runs with a conservation limit of 50 females and catch in year y equal to the difference between spawners in year $y - 1$ and the CL. The bottom frames show catches under constant effort (red) and CL driven (blue) management.

after a weak one, produces periods of high-frequency population oscillations, which are (not unexpectedly) less persistent in the case where the unmanaged population time-series would show strong serial correlation. In the weak correlation case the induced fluctuations are severe enough to repeatedly drive single pseudo lineages to extinction, requiring that they be (slowly) replenished by leakage from their cousins spawning in nearby sequences of years.

Examination of the catch time series also shown in Fig. 7 exposes the full inefficiency of the CL driven management policy. In the strong serial correlation case the mean catch is considerably more variable than the constant effort catch and its long-run average is rather smaller, despite a small increase in the long-run average population. In the weak correlation case, the CL driven policy actually manages to reduce the long-run mean spawning stock to below 70 females, and reduce the long-run average catch to 21 fish per year (compared to nearly 80 under the constant effort policy). The reason for this reduction is the policy's tendency to produce near extinction of certain pseudo-lineages which in turn imply multiple years in which the fishery is completely shut (an outcome likely to imply disproportionate financial damage to the industry !).

3. A prototype genetic model for a single deme

We now construct an extended model which assumes that sea-age at return to the river is determined by a single genetic locus at which there are two alleles (\mathcal{G}, \mathcal{M}). Wild salmon are diploid, so we distinguish three genotypes, $\mathcal{G}\mathcal{G}$, $\mathcal{G}\mathcal{M}$ and $\mathcal{M}\mathcal{M}$, which for the sake of compactness we hereafter denote as G , X and M . We assume that the \mathcal{M} allele is dominant, implying that only the G type returns as a grilse and both the homozygote M and heterozygote X types return after multiple sea-winters. To facilitate a stochastic formulation we treat males and females independently; using N_y^{qs} to denote the number of individuals of type q ($\in \{G, X, M\}$) and sex s ($\in \{f, m\}$) spawning in year y .

Our assumptions imply that individuals of a given genotype spend a specific number of years at sea, but they may live in the river for different periods before emigrating to sea, and hence may return at a variety of ages (since spawning). If c_y^{qsa} denotes the number of individuals of type q , sex s and age a who return to the coast in year y , then the total number of type q individuals with sex s returning in year y , which we write C_y^{qs} , is

$$C_y^{qs} = \sum_{a=0}^{a_{max}} c_y^{qsa}, \quad (10)$$

where a_{max} is the maximum possible age at return.

If an expected fraction E_y^{qs} of these returners escape exploitation and spawn, and the actual number of survivors is negative binomially distributed around the implied mean with shape factor θ_E^{qs} then the number of spawners of type q and sex s in year y is

$$N_y^{qs} = B_n([E_y^{qs} C_y^{qs}], \theta_E^{qs}), \quad (11)$$

where $B_n(\mu, \theta)$ is a negative binomially distributed random variable with mean μ and shape factor θ .

To relate the number of returners to reproductive activity we first assert that spawning in year y gives rise to R_y^{qs} individuals of genotype q and sex s . We then write the expected proportion of this group who survive to return to the coast at any age as S_y^{qs} and the expected proportion of these survivors who arrive aged a as P_a^{qs} . Hence, in year y , the expected number of type q arrivals with sex s and age a is $P_a^{qs} S_{y-a}^{qs} R_{y-a}^{qs}$. Assuming that the actual number of arrivals is negative binomially distributed with shape factor θ_S^{qs} , this implies that the actual number of arrivals that year, c_y^{qsa} , is

$$c_y^{qsa} = B_n([P_a^{qs} S_{y-a}^{qs} R_{y-a}^{qs}], \theta_S^{qs}). \quad (12)$$

To relate net reproductive outputs $\{R_y^{qs}\}$ to numbers of spawners $\{N_y^{qs}\}$ we first assert that all males involved in year y spawning have a chance of fertilising any ovum which is proportional to the number of sperm they contribute to the ‘pool’. Hence, if the relative fecundity of a type q male is ρ^q , the probability, ϕ_y^q , that any given ovum is fertilised by a type q male is

$$\phi_y^q = \frac{\rho^q N_y^{qm}}{T_y} \quad \text{where} \quad T_y \equiv \sum_{\text{all } q} \rho^q N_y^{qm} \quad (13)$$

We next assume that the group of type q females spawning in year y produce O_y^q ova which will survive to the time at which we count new recruits. The latest life-history

stage at which we might envisage such recruits entering the population is smolting and emigration to sea – a stage at which we can safely assume that the sex-ratio is the same as that observed for smolting coho salmon, namely 1:1. Hence, since fertilised eggs must have a 1:1 sex ratio we can see that independent of the exact stage at which recruits join the population, their numbers are related to the fertilisation probabilities, $\{\phi_y^q\}$, and the female reproductive outputs, $\{O_y^q\}$, by

$$R_y^{qs} = \begin{cases} \frac{1}{2} [O_y^G (\phi_y^G + \frac{1}{2}\phi_y^X) + O_y^X (\frac{1}{2}\phi_y^G + \frac{1}{4}\phi_y^X)] & \text{if } q = G \\ \frac{1}{2} [\frac{1}{2}O_y^X + O_y^G (\phi_y^M + \frac{1}{2}\phi_y^X) + O_y^M (\phi_y^G + \frac{1}{2}\phi_y^X)] & \text{if } q = X \\ \frac{1}{2} [O_y^M (\phi_y^M + \frac{1}{2}\phi_y^X) + O_y^X (\frac{1}{2}\phi_y^M + \frac{1}{4}\phi_y^X)] & \text{if } q = M \end{cases} \quad (14)$$

To complete the model we need to relate the female outputs, $\{O_y^q\}$, to the numbers of participating females, $\{N_y^{qf}\}$. However, since a number of distinct formulations can be accommodated in the basic framework outlined here, we defer the description of this model component to the next section.

4. An exemplary application

4.1. The independent territories model of grilse/MSW interaction

As a trial implementation of the structure described above we adopt a formulation for the female reproductive output taken from a deterministic model of the genetics of grilse/MSW coexistence described and analysed in a previous report. We assume that female grilse compete only with each other – for example, because they utilise different habitat from female MSW fish. Female X and M types are assumed to be functionally identical and thus form a single reproducing group. We adopt a Ricker form of stock recruitment relation for each reproducing group, and thus write the expected reproductive output for grilse (\widehat{T}_y^G) and MSW fish (\widehat{T}_y^M) as

$$\widehat{T}_y^G = T_{max}^G \left(\frac{N_y^{Gf}}{F_{max}^G} \right) \exp \left(1 - \frac{N_y^{Gf}}{F_{max}^G} \right) \quad (15)$$

and

$$\widehat{T}_y^M = T_{max}^M \left(\frac{N_y^{Xf} + N_y^{Mf}}{F_{max}^M} \right) \exp \left(1 - \frac{N_y^{Mf} + N_y^{Xf}}{F_{max}^M} \right) \quad (16)$$

To model variability about this expected output we assume negative binomial distributions with shape factors θ_T^G and θ_T^M respectively and hence write the actual outputs of surviving offspring (T_y^G and T_y^M) as

$$T_y^q = B_n(\widehat{T}_y^q, \theta_T^q) \quad q \in \{G, M\}. \quad (17)$$

Finally we assume that all members of the MSW group are functionally identical and that the fate of the offspring of the homo- and hetero-zygote sub-groups is highly correlated. Thus we write the offspring outputs of the three maternal genotypes as

$$O_y^G = T_y^G, \quad O_y^X = \left(\frac{N_y^{Xf}}{N_y^{Xf} + N_y^{Mf}} \right) T_y^M, \quad O_y^M = \left(\frac{N_y^{Mf}}{N_y^{Xf} + N_y^{Mf}} \right) T_y^M. \quad (18)$$

Observation of sea survival is difficult, but we know that the sex-ratio of returners is both different from 1:1 and variable between sub-catchments (e.g. upland/lowland regions within a single catchment). Hence we specify the expected sea-survivals in terms of an expected value across both sexes (\widehat{S}^G for grilse and \widehat{S}^M for MSW fish) and a corresponding proportion female (η^G and η^M respectively). In terms of these quantities, it is straightforward to see that

$$S^{qs} = \begin{cases} 2\eta^G \widehat{S}^G & \text{if } q = G \text{ and } s = f \\ 2(1 - \eta^G) \widehat{S}^G & \text{if } q = G \text{ and } s = m \\ 2\eta^M \widehat{S}^M & \text{if } q \in \{X, M\} \text{ and } s = f \\ 2(1 - \eta^M) \widehat{S}^M & \text{if } q \in \{X, M\} \text{ and } s = m \end{cases} \quad (19)$$

The complete parameter set, together with values yielding steady states which mimic the abundances observed in the Girnock Burn for the periods 1970-79 and 1990-99, and assume that both grilse and MSW fish can spend either three or four years (N.B. from *spawning*, not hatch) in the river with equal probability, are shown in Table 1 below.

Table 1: Parameters for Girnock Burn during the periods 1970-1979 and 1990-99.

Param	Symbol	Unit	Grilse		Multi seawinter	
			1970-79	1990-99	1970-99	1990-99
Max. surviving offspring	T_{max}	Offspring	400	400	4000	4000
Female population scale	F_{max}	Females	8	8	80	80
Reproduction neg. bin. shape	θ_T	–	15	15	15	15
Average sea survival	\widehat{S}	–	0.08	0.06	0.05	0.03
Proportion returners female	η	–	0.3	0.3	0.6	0.6
Sea survival neg.bin. shape	θ_S	–	300	300	300	300
Exploitation escape prob.	E	–	0.5	0.5	0.6	0.6
Exploitation neg.bin. shape	θ_E	–	300	300	300	300
Return probability (age 1)	P_1	–	0	0	0	0
Return probability (age 2)	P_2	–	0	0	0	0
Return probability (age 3)	P_3	–	0	0	0	0
Return probability (age 4)	P_4	–	0.5	0.5	0	0
Return probability (age 5)	P_5	–	0.5	0.5	0.5	0.5
Return probability (age 6)	P_6	–	0	0	0.5	0.5
Return probability (age 7)	P_7	–	0	0	0	0

4.2. Implementation

The code to implement this model is given in Appendix B.3. It can be run deterministically or stochastically, but even in its stochastic guise it can simulate 10,000 years in about 3 seconds. It can thus make 1000 replicate 100 year runs in about 30 seconds – implying that evaluating the probability distribution of medium-term outcomes is entirely practical.

4.3. Stationary States

We first explore the deterministic behaviour of the model with parameters chosen to mimic the observations for the Girnock Burn during the 1970's. We illustrate a 100 year

deterministic run in Fig. 8, where we see the system settle rapidly to a stationary state with all genotypes at positive values – thus representing a stable genetic polymorphism.

We note that although the \mathcal{MM} and \mathcal{GM} genotypes settle to their equilibrium values within about a decade (two generations), the \mathcal{GG} genotype takes nearly the full 100 years (20 generations) to settle. We further remark that (as required by the model parameters) the grilse are predominantly male while the sex-ratio of the MSW fish is slightly female biased.

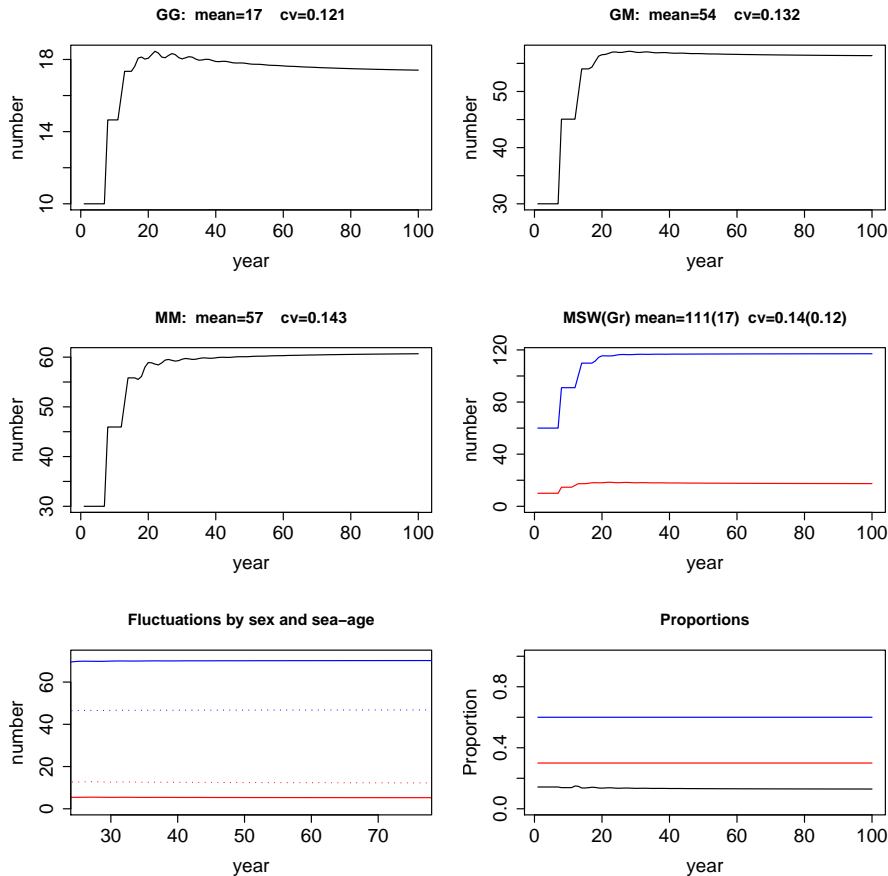


Figure 8: *Deterministic behaviour of the independent territories variant of the single deme model with parameters given for 1970-79 in Table 1. The top two frames and the left middle frame show the frequencies of \mathcal{GG} , \mathcal{GM} and \mathcal{MM} genotypes moving from a non-equilibrium initial state to a long-run stationary state indicating a stable polymorphism. The right-hand middle frame shows the numbers of functional grilse (red) and MSW fish (blue). The bottom left-hand frame shows grilse and MSW fish decomposed into males (dotted) and females (continuous) with grilse in red and MSW in blue as before. The lower right-hand frame shows proportions of total returners who are grilse (black) and proportions of grilse (red) and MSW (blue) who are female.*

In Fig. 9 we illustrate the last 1000 years of a 1500 year stochastic run with the same parameters; the first 500 years being discarded since we are interested in the properties of the statistically stationary state which our deterministic run leads us to expect will be reached after a few tens of years.

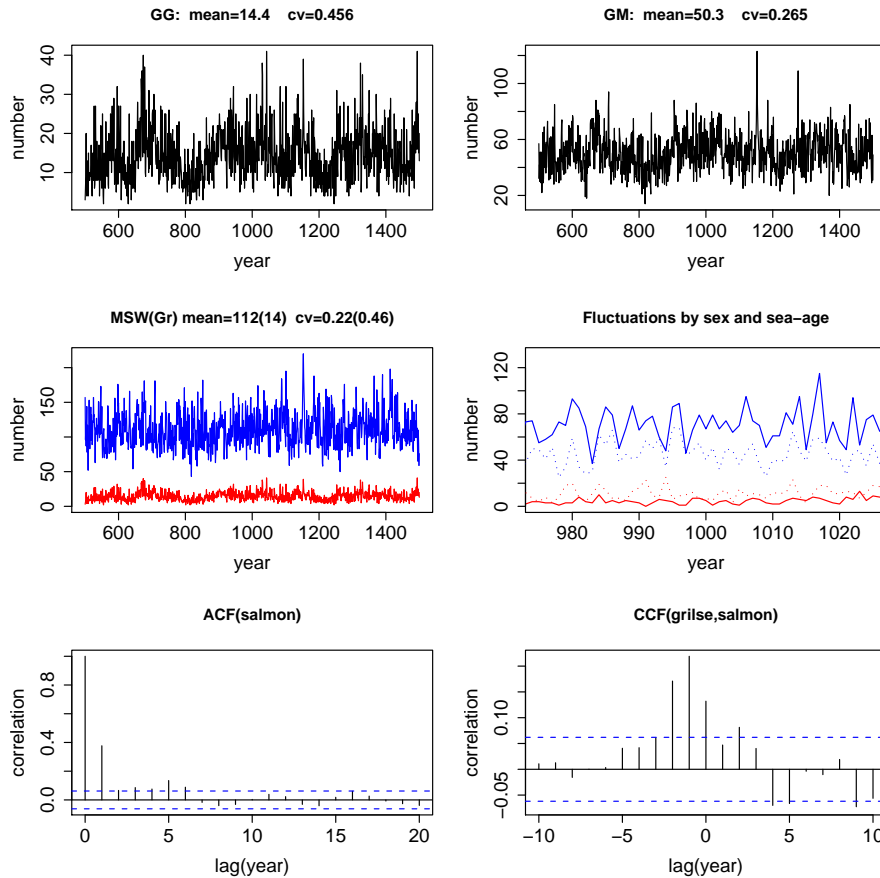


Figure 9: *Stochastic behaviour of the independent territories variant of the single deme model with parameters given for 1970-79 in Table 1.* The top two frames show statistically stationary fluctuations in the frequencies of GG , GM genotypes. The left-hand middle frame shows similarly statistically stationary fluctuations in the numbers of functional grilse (red) and MSW fish (blue). The right-hand middle frame shows a 50-year times series of fluctuations in grilse and functional MSW fish decomposed into males (dotted) and females (continuous) with grilse in red and MSW in blue as before. The lower left-hand frame shows the autocorrelation function for the fluctuations in MSW numbers and the lower right hand frame shows the cross-correlation between grilse and salmon numbers.

It is clear from the first three frames of the figure (the top row and the LH middle) that the system is indeed in a statistically stationary state – although we note the the time series for the GG genotype shows periods of as much as a century with apparently secular trends (of both signs !). Although the mean population abundances are clearly close (but by no means identical) to the deterministic steady state, we note that the short term (i.e. 10 year) mean abundances (particularly for grilse) may bear little relation to the long-term mean value.

The most interesting outcomes of the run are shown in the last three frames. The 50-year times series segment shown in the R.H. middle frame illustrates the more formal analysis represented by the correlation functions shown in the bottom two frames. We see that despite male and female survival being entirely uncorrelated (as well as sex-specific) the male and female numbers of both functional types show correlated fluctuations.

The fluctuations in grilse numbers are significantly correlated with MSW numbers at a lag of -1 year – demonstrating that large MSW spawning numbers are accompanied by high grilse production. This is perhaps less surprising than it might first seem, because a high proportion of the functional MSW (model) population are heterozygotes, a quarter of whose matings produce grilse.

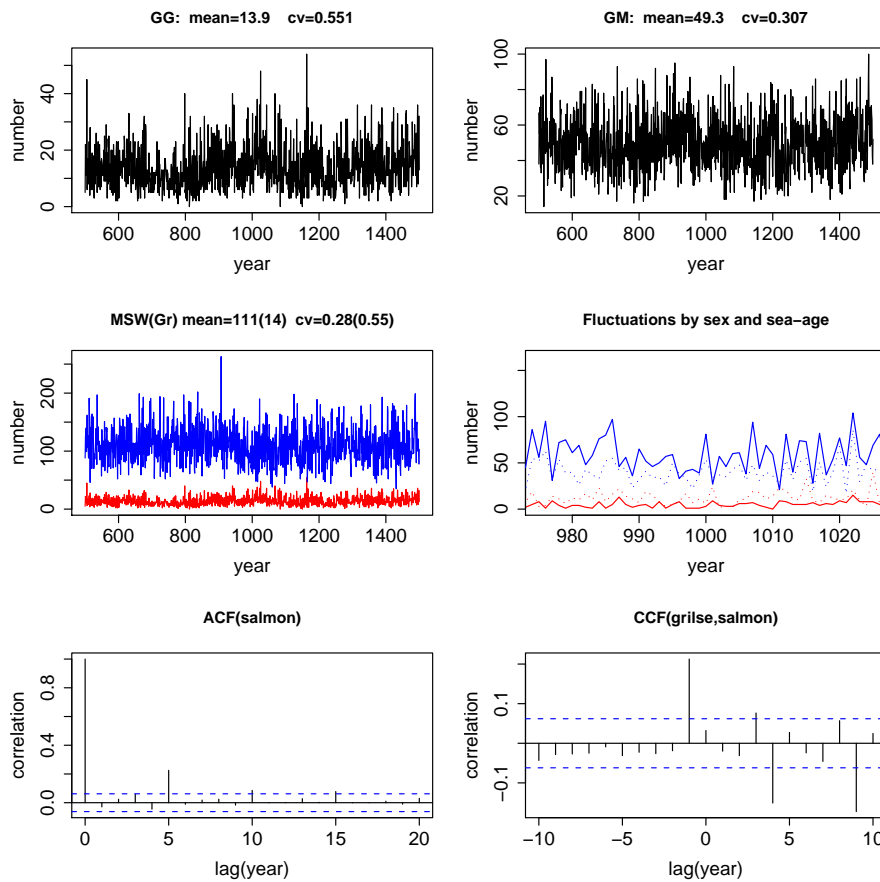


Figure 10: *Stochastic behaviour of the independent territories variant of the single deme model with parameters given for 1970-79 in Table 1 except that all grilse return aged 4 and all MSW fish return aged 5. The top two frames show statistically stationary fluctuations in the frequencies of GG, GM genotypes. The left-hand middle frame shows similarly statistically stationary fluctuations in the numbers of functional grilse (red) and MSW fish (blue). The right-hand middle frame shows a 50-year times series of fluctuations in grilse and functional MSW fish decomposed into males (dotted) and females continuous with grilse in red and MSW in blue as before. The lower left-hand frame shows the autocorrelation function for the fluctuations in MSW numbers and the lower right hand frame shows the cross-correlation between grilse and salmon numbers.*

We also note that the salmon (MSW) time series shows just significant serial correlation at lags of five and six years, and quite strong (nearly 40%) correlation at a one year lag. The first of these correlations, which plays a key role in generating the rather realistic fluctuation pattern (RH middle frame), reflects the generation time, while the second (which would be *essential* for management actions based on population estimates for previous years) is the outcome of the dispersion of return ages. Removing this dispersion

(see Fig. 10) strengthens the correlation at 5 years but entirely removes that at one year. Conversely, increased return age dispersion (not illustrated) would produce (weaker) serial correlation over a wider range of years.

5. Stochastic Projection

The computational efficiency of the prototype model described here readily lends itself to stochastic population projection. In Fig. 11 we illustrate a scenario test in which it is assumed that prior to year zero the system parameters are those given in Table 1 for the period 1970-79, while after that time they are those given in the same Table for the period 1990-99.

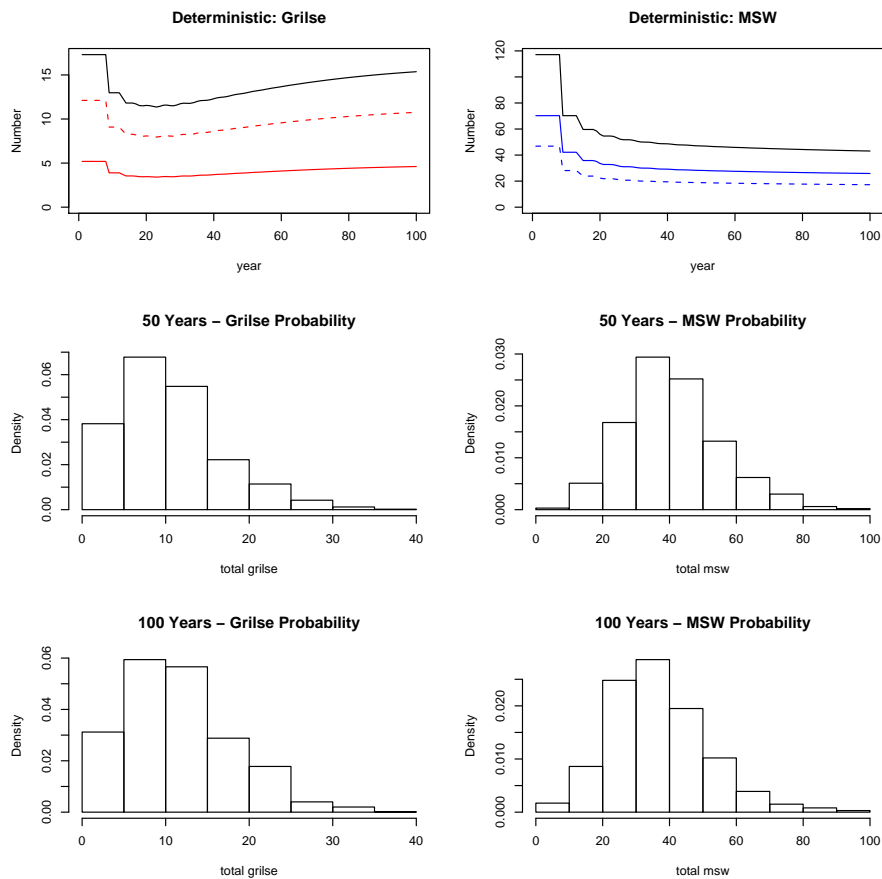


Figure 11: 100-year stochastic projection of the independent territories variant of the single deme model spun up with parameters given for 1970-79 in Table 1, assumed to have parameters given for 1990-99 in Table 1 from $t = 0$ onwards and system state held at the earlier steady state until year 7. The top two frames show the deterministic predictions for the abundance of grilse (left frame, total=black, male=dotted, female=continuous red) and MSW fish (total=black, male=dotted, female=continuous blue). Middle and lower pairs of frame show probability distributions for grilse (left) and MSW (right) at 50 (middle) and 100 (lower) years.

In this run we assume that at year zero the system is in the deterministic steady state

appropriate to the initial parameters. To simulate the effect of individuals returning to spawn during the first seven years of the run, who will mainly have been spawned before year zero, we hold the spawning population at its prior steady state until year eight. Once the system is released, its deterministic state relaxes to a stationary value appropriate to the new parameters (top two frames). However, we note while the MSW abundance reaches this new equilibrium quickly, the grilse first undershoot their final abundance and then increase slowly to a final equilibrium little below their 1970-79 state.

As an illustration of the possibilities implied by stochastic simulation, we have performed 1000 replicate stochastic projections of the step response and plotted the probability distributions for the spawning populations at 50 and 100 years. As we would expect, the population abundance is widely dispersed (although with these parameters, no replicate becomes extinct!). However, with a little care we can see that although the MSW distributions for 50 and 100 years are distinguished only by slightly greater dispersion at 50 years, the mean grilse population at 50 years is clearly lower than that at 100 years.

6. Conclusions

Our investigations of data from three distinct locations have demonstrated that robustly non-linear relationships between spawning stock and some measure of recruitment to the population are common (perhaps universal) in populations of Atlantic salmon. However, despite the abundant nature of at least some of these datasets it is clear that the details of the shape of these relations (especially at low spawning stock) are not well determined by currently available data. Since the low-stock shape of the stock-recruitment curve plays a central role in determining population persistence, our first conclusion is that mechanistic understanding of the mechanisms(s) which drive these non-linear relationships is essential to future progress.

In addition to the deterministic non-linearity, all observed stock-recruitment relations show high levels of year on year variability. To investigate the role played by such variability in driving year on year fluctuations in salmon populations, we have constructed a series of strategic stochastic population models which operate on both a generation by generation and on a year by year basis.

These models demonstrate that dispersion in absolute age at return plays a key role in determining the serial correlation between spawning stock in successive years, which is a central requirement for the application of short term management actions. For a model parameterised with a realistic age-at-return dispersion we investigated the application of management policies simplistically based on catch limits determined from prior year's spawning stock, and showed that the effects of such policies are almost universally to increase the amplitude of population fluctuations and decrease medium term fisheries yields.

To investigate the robustness of these conclusions we formulated an extended model incorporating increased biological realism (males and females, heritable one and two sea-winter return). This extended model clearly showed that our earlier conclusions are robust. In addition it demonstrated that this (still rather simplistic) population representation is capable of mimicking many of the qualitative features of long-term observations such as those made at the Girnock Burn over the period 1967-2003. We thus believe that this representation has the capacity to form the basis of an operational model for application to salmon population management.

Appendix

A. Data fits

A.1. Modified Ricker: Girnock Spawner → Fry

Figure 12: Girnock Spawner-Fry Fits. a) Best fit with data. b) Standardised residuals c) Best fit with 95% conf. lims d) Data with implied mean (solid), one s.d. (dashed) and two s.d. (dotted).

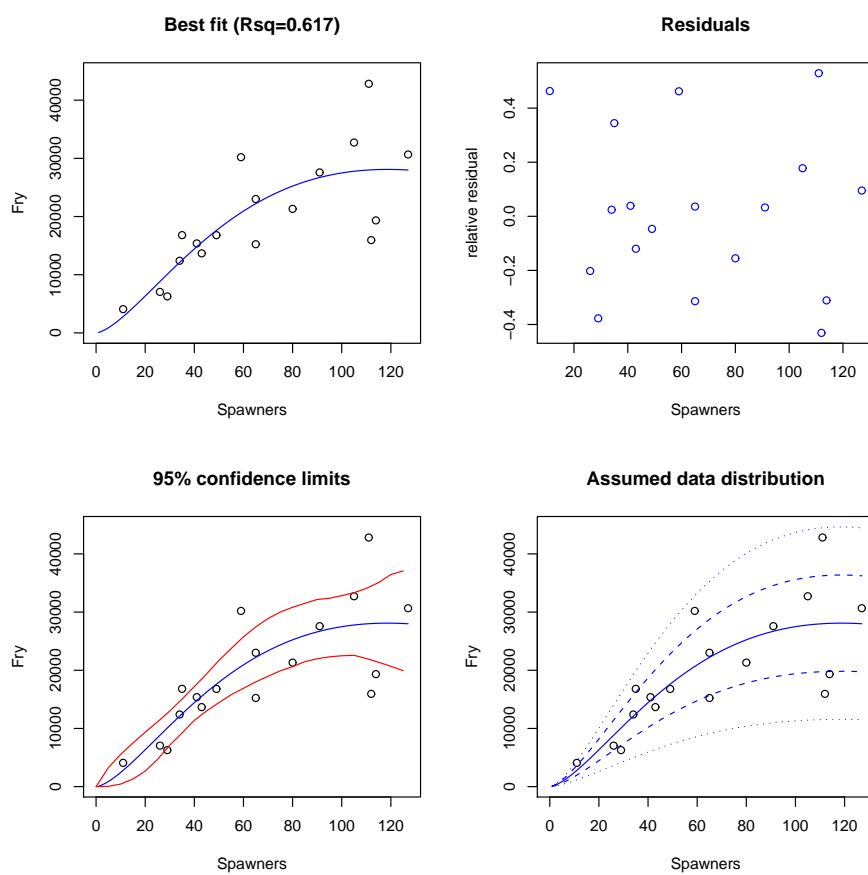


Figure 13: *Girnock Spawner-Fry Parameters. Top – histograms. Bottom – scattergrams.*

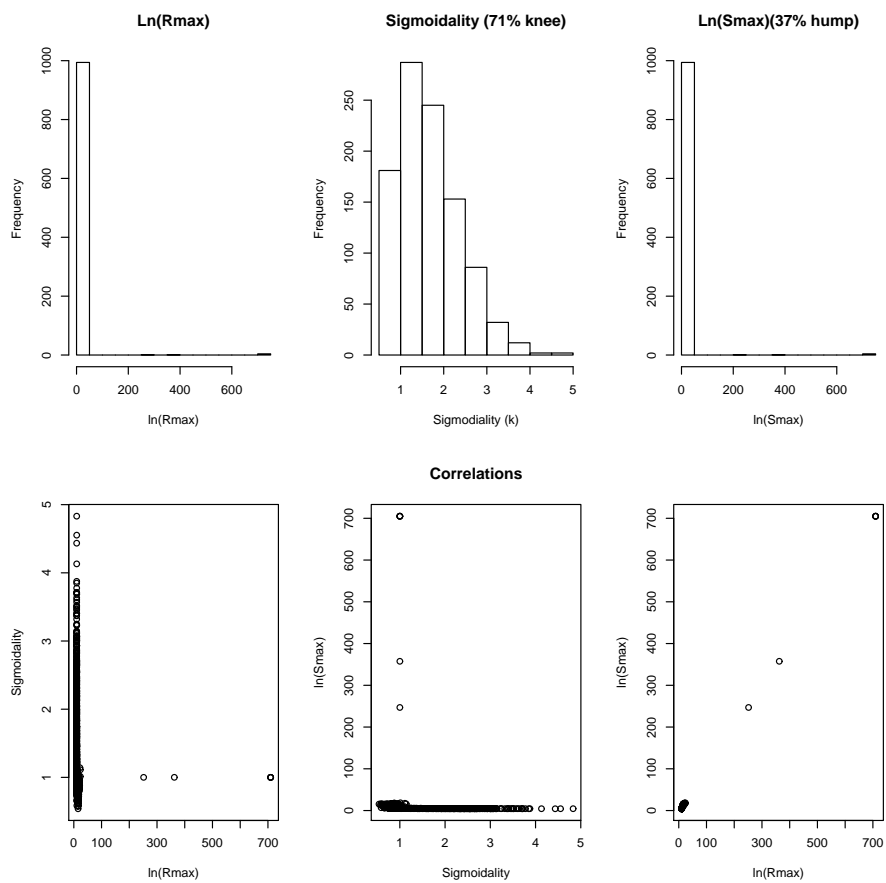
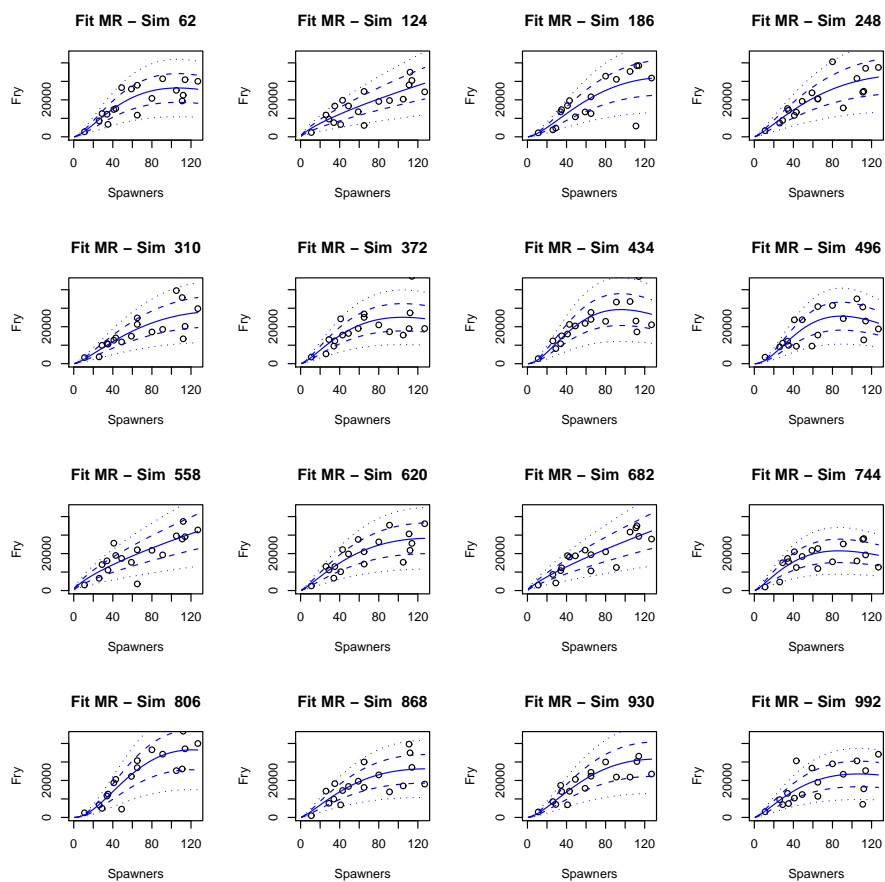


Figure 14: *Girnock Spawner-Fry Simulations*

A.2. Sigmoidal Ricker: Girnock Spawner → Smolt

Figure 15: *Girnock Spawner-Smolt Fits*. a) Best fit with data. b) Standardised residuals c) Best fit with 95% confidence limits d) Data with implied mean (solid), one s.d. (dashed) and two s.d. (dotted).

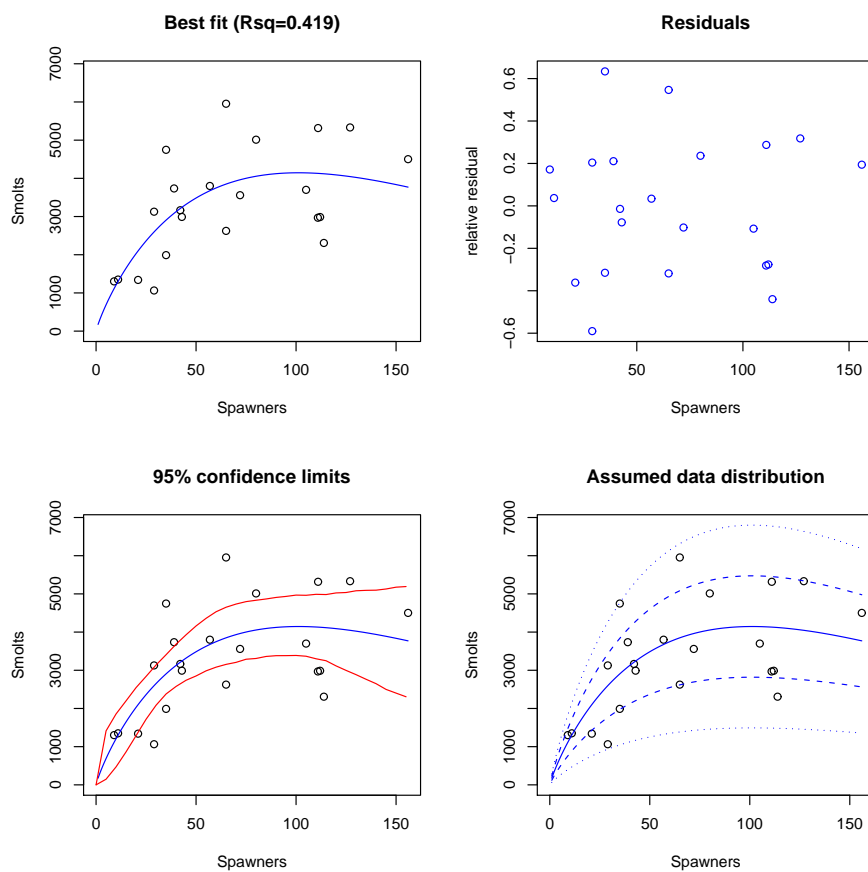


Figure 16: *Girnock Spawner-Smolt Parameters*. Top – histograms. Bottom – scattergrams.

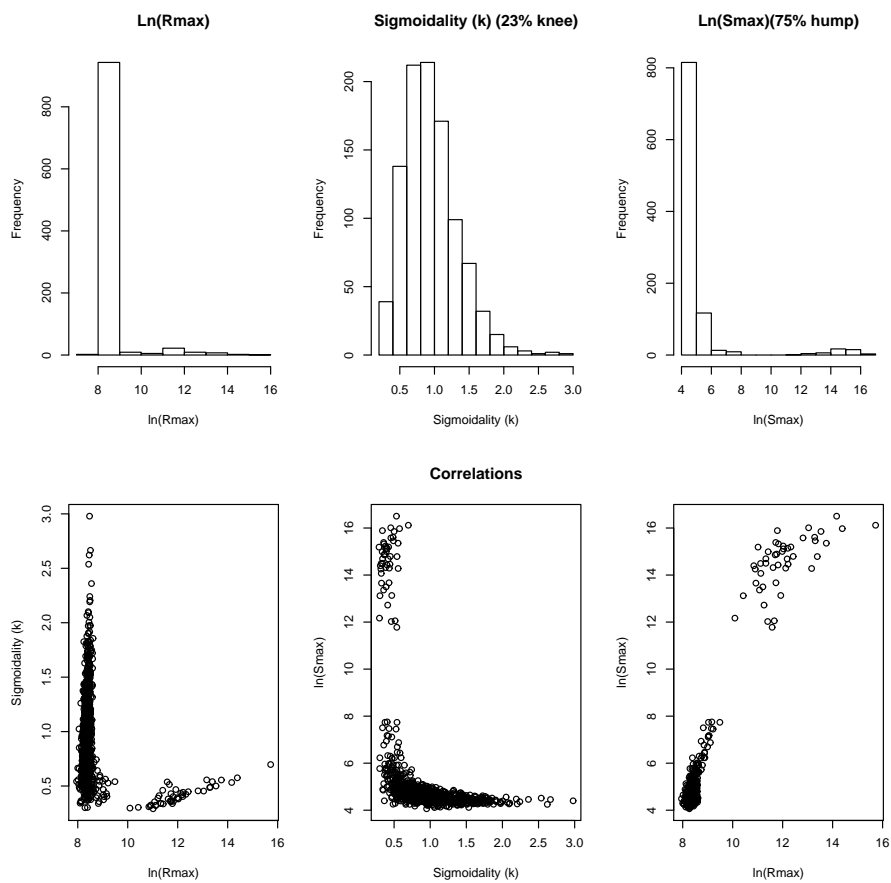
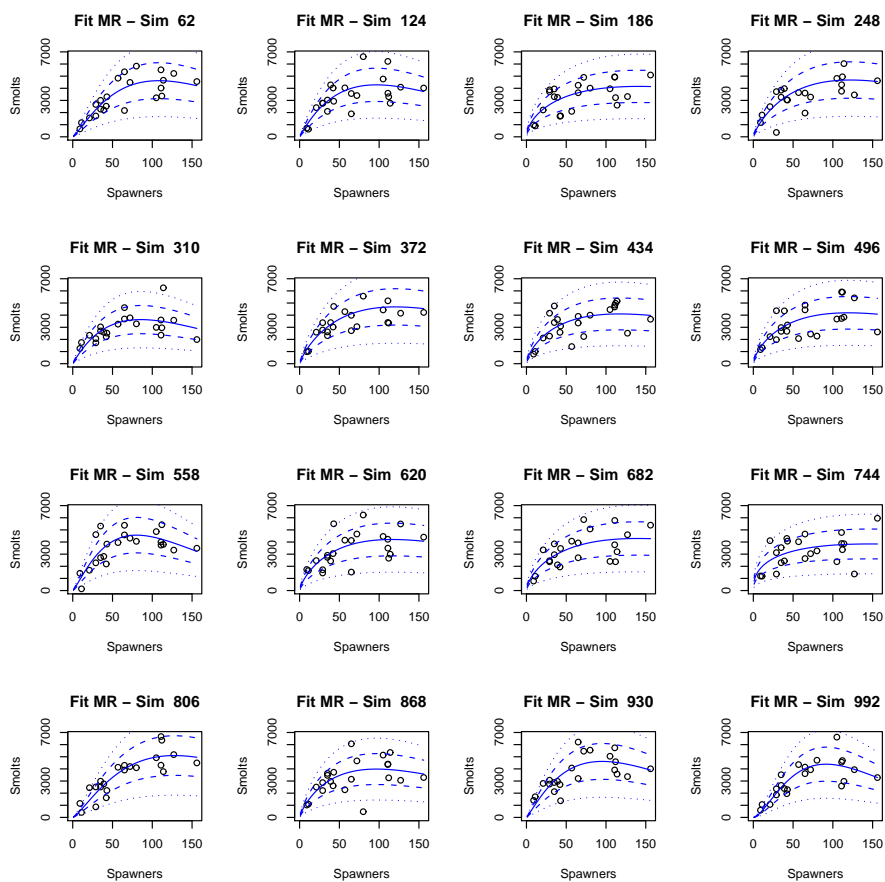


Figure 17: *Girnock Spawner-Smolt Simulations*

A.3. Sigmoidal Ricker: Bush Ova \rightarrow Smolt

Figure 18: Bush Ova-Smolt Fits. a) Best fit with data. b) Standardised residuals c) Best fit with 95% confidence limits d) Data with implied mean (solid), one s.d. (dashed) and two s.d. (dotted).

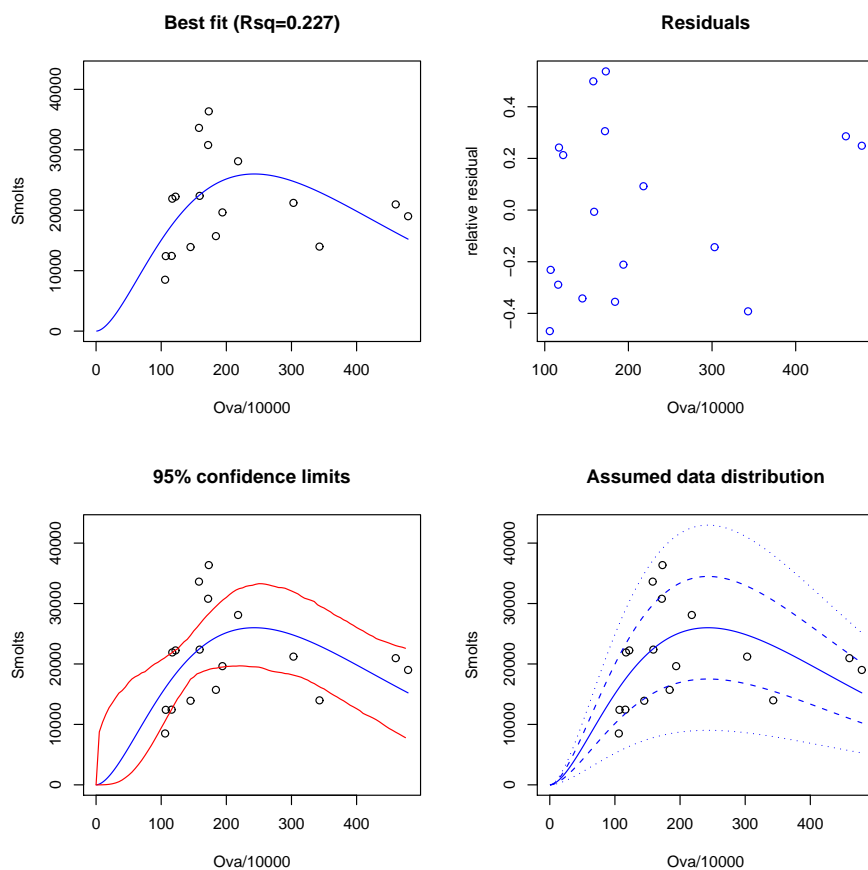


Figure 19: *Bush Ova-Smolt Parameters. Top – histograms. Bottom – scattergrams.*

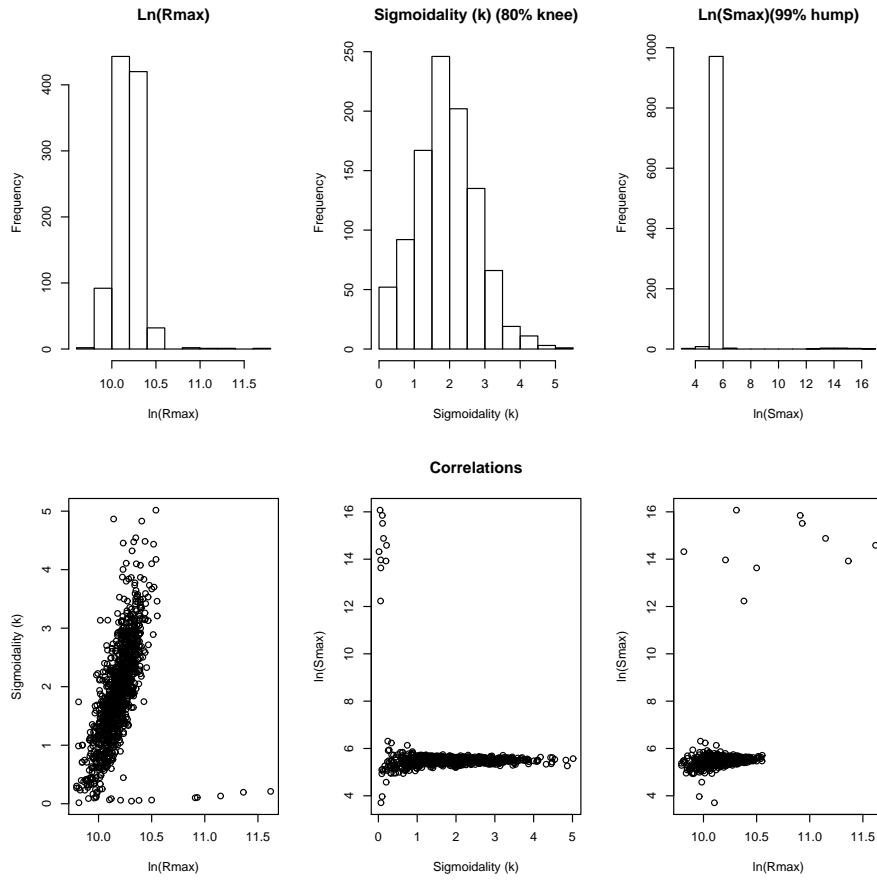
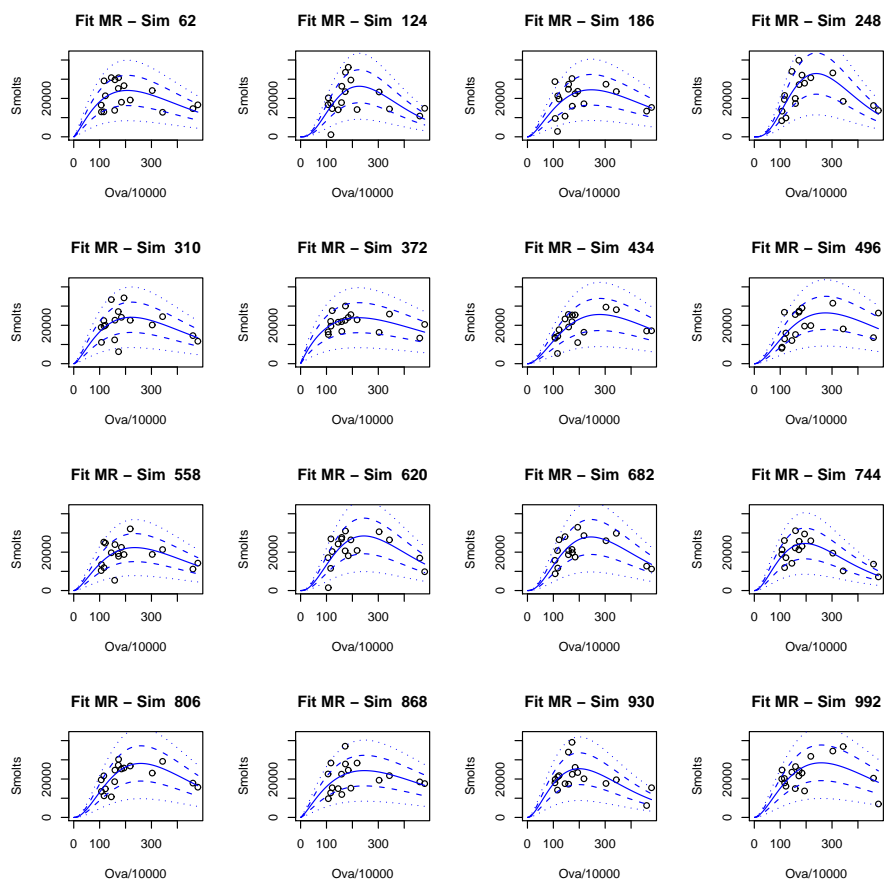


Figure 20: *Bush Ova-Smolt Simulations*

A.4. Sigmoidal Ricker: N. Esk Spawner → Pre-fisheries Returner

Figure 21: N. Esk Adult-Adult Fits. a) Best fit with data. b) Standardised residuals c) Best fit with 95% confidence limits d) Data with implied mean (solid), one s.d (dashed) and two s.d. (dotted).

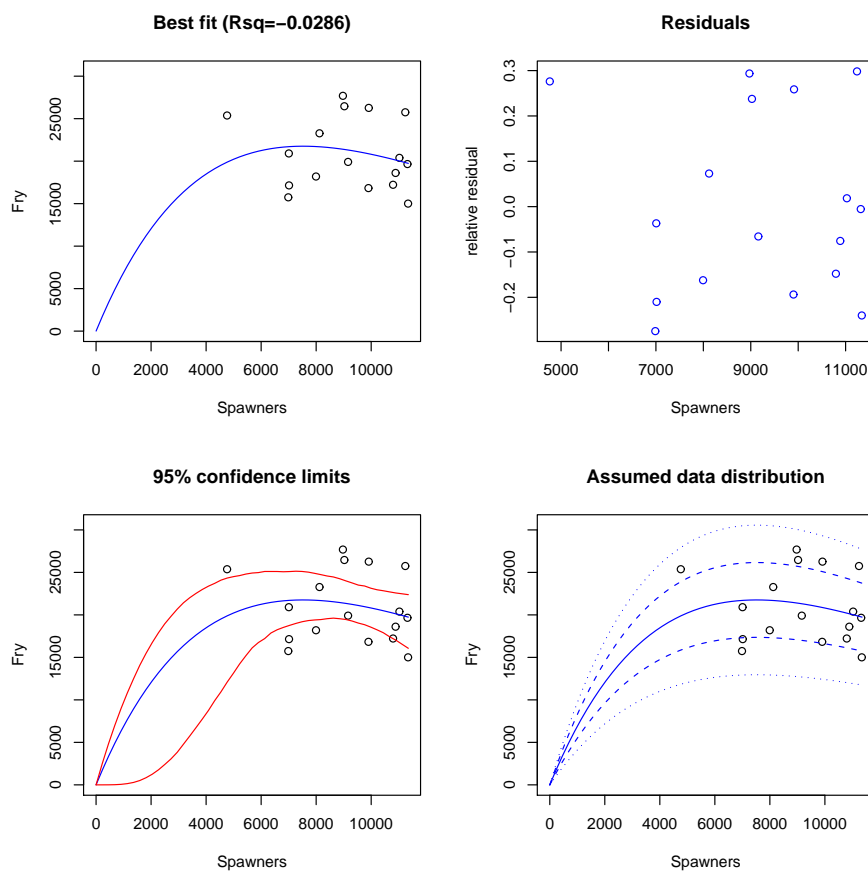


Figure 22: *N. Esk* Adult-Adult Parameters. Top – histograms. Bottom – scattergrams.

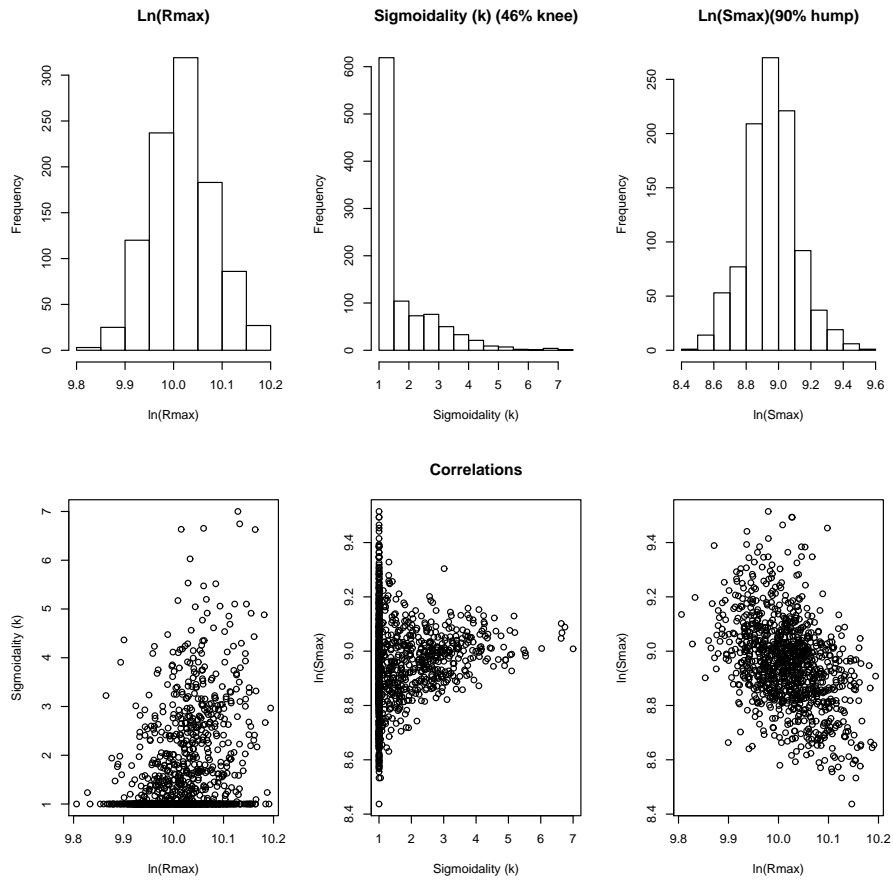
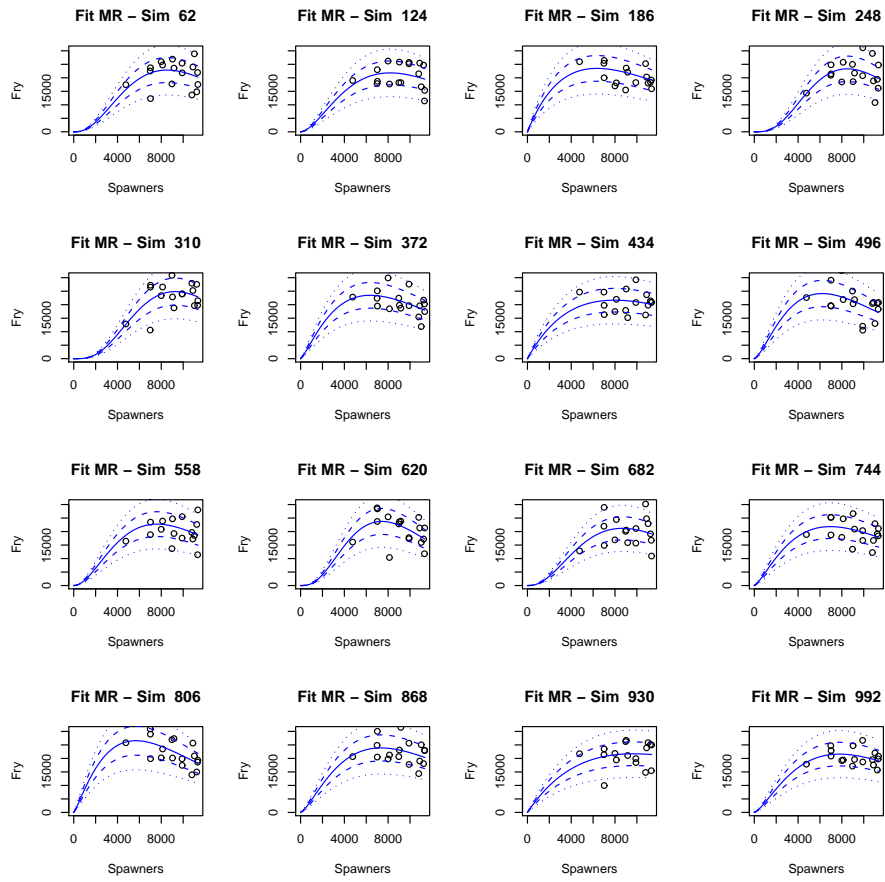


Figure 23: *N. Esk* Adult-Adult Simulations

A.5. Broken Stick: Girnock Spawner \rightarrow Fry

Figure 24: Girnock Spawner-Fry Fits. a) Best fit with data. b) Standardised residuals c) Best fit with 95% confidence limits d) Data with implied mean (solid), one s.d. (dashed) and two s.d. (dotted).

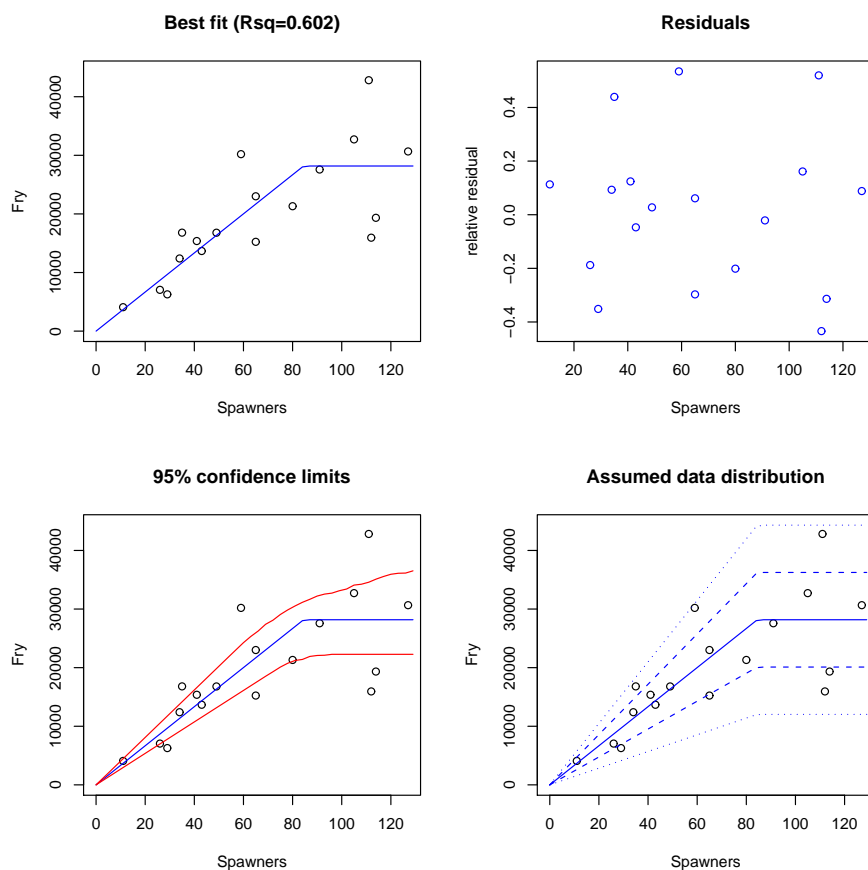


Figure 25: *Girnock Spawner-Fry Parameters*. Top – histograms. Bottom – scattergrams.

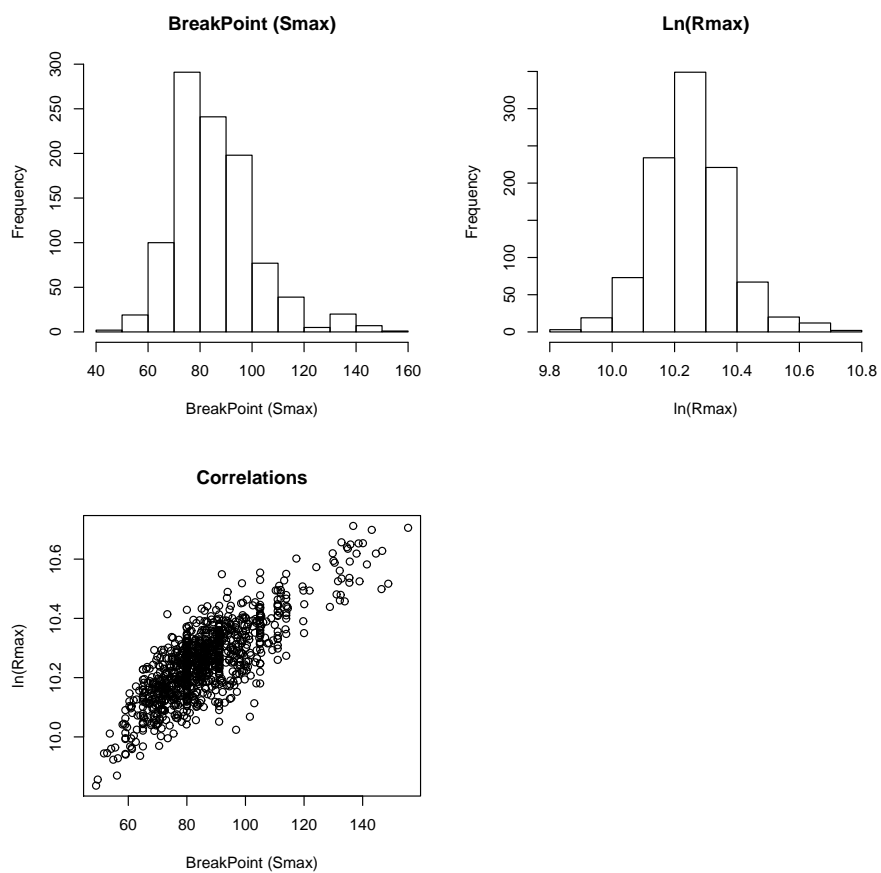
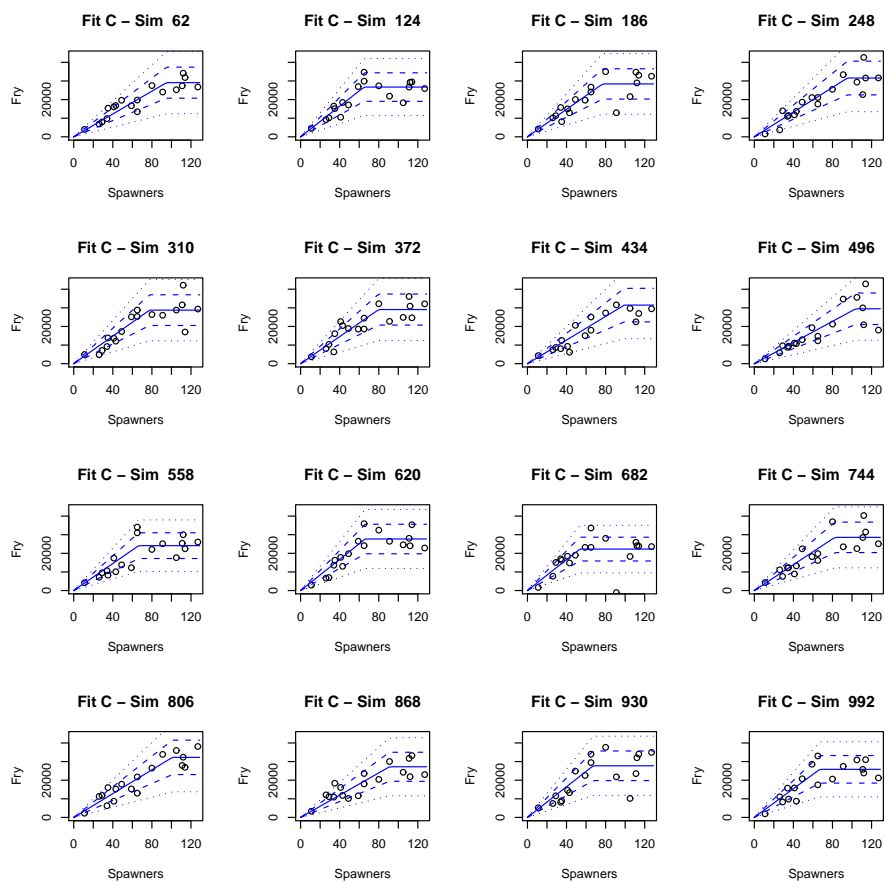


Figure 26: *Girnock Spawner-Fry Simulations*

A.6. Broken Stick: Girnock Spawner → Smolt

Figure 27: *Girnock Spawner-Smolt Fits*. a) Best fit with data. b) Standardised residuals c) Best fit with 95% confidence limits d) Data with implied mean (solid), one s.d. (dashed) and two s.d. (dotted).

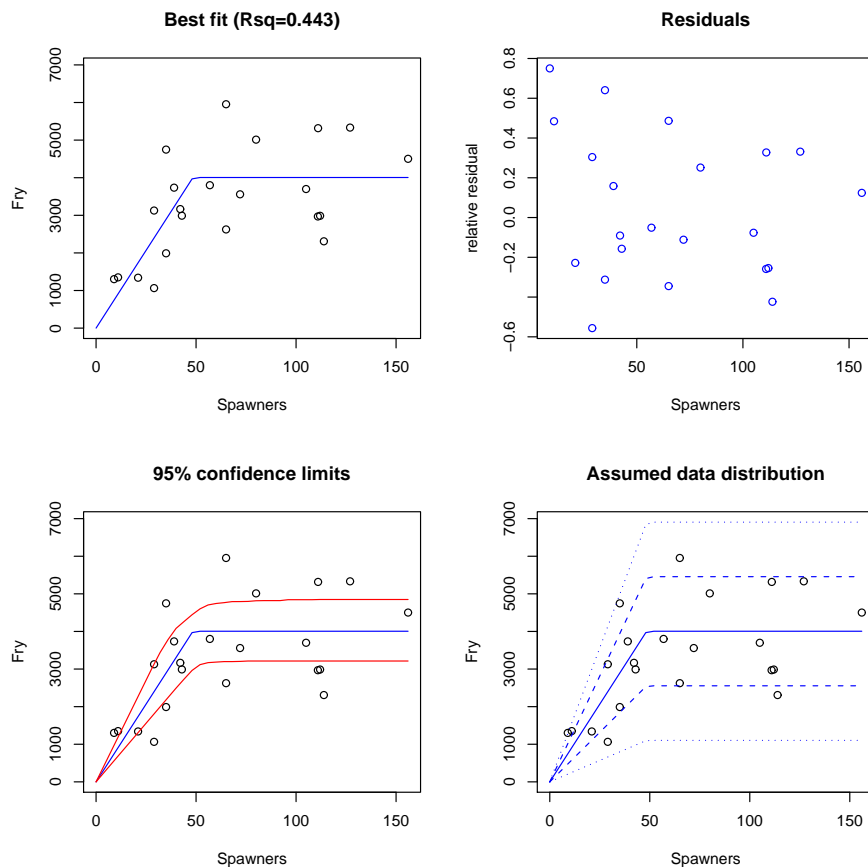


Figure 28: *Girnock Spawner-Smolt Parameters. Top – histograms. Bottom – scattergrams.*

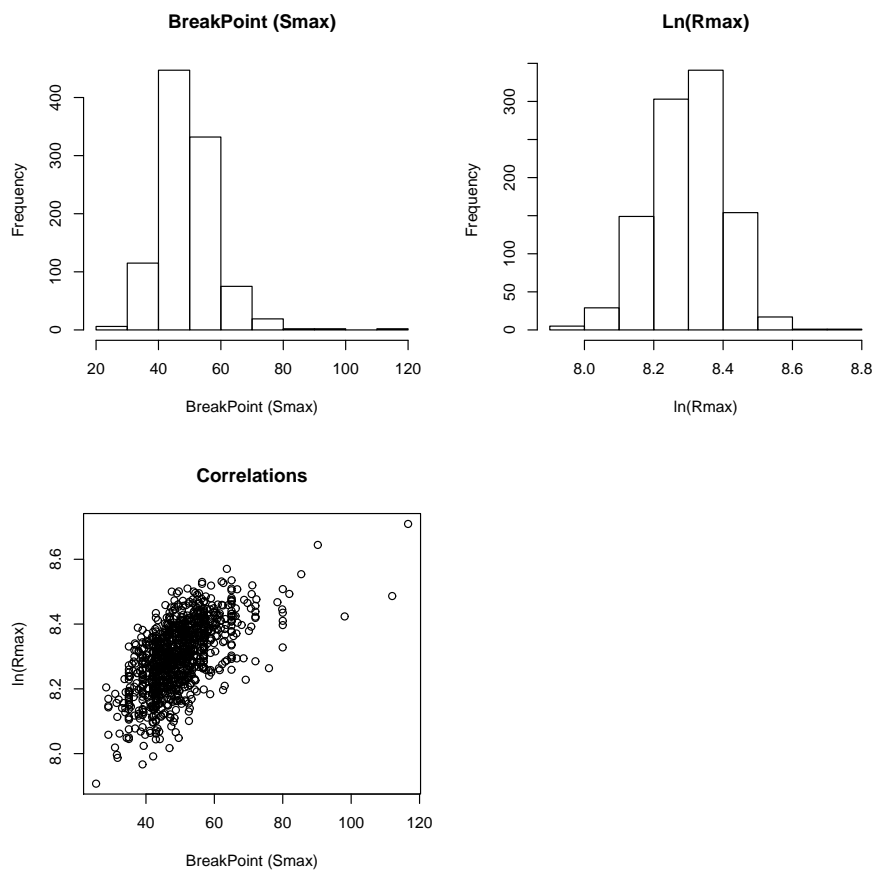
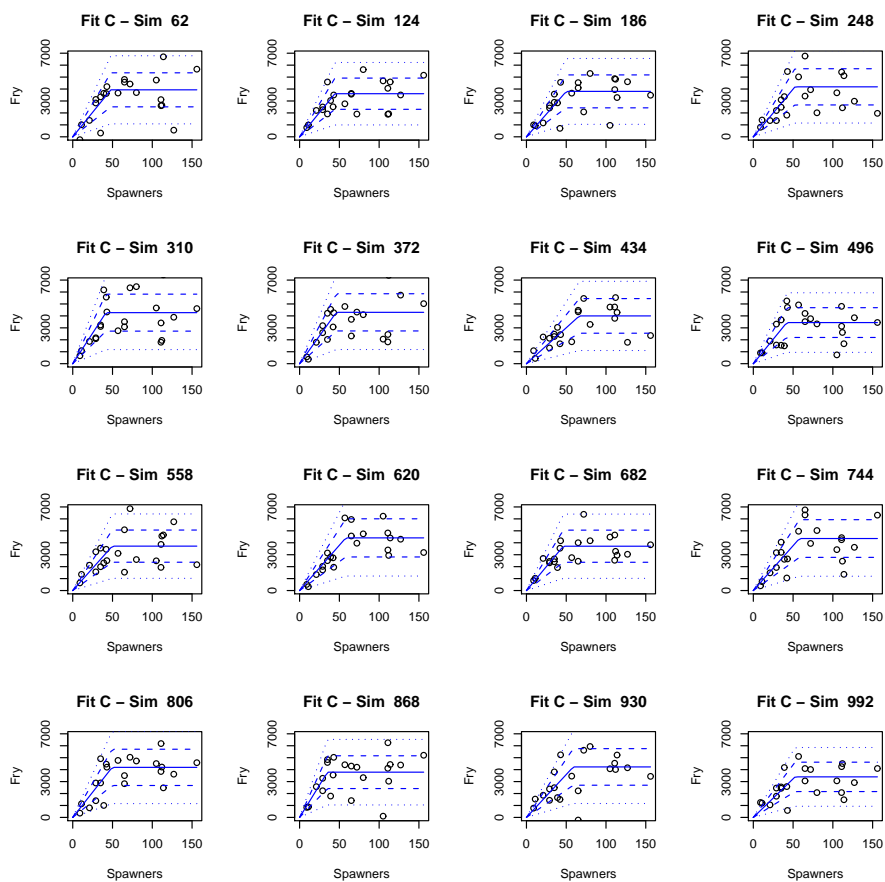


Figure 29: *GirnockSpawner-Smolt Simulations*

A.7. Straight line: Bush Ova → Smolt

Figure 30: Bush Ova-Smolt Fits. a) Best fit with data. b) Standardised residuals c) Best fit with 95% confidence limits d) Data with implied mean (solid), one s.d (dashed) and two s.d. (dotted).

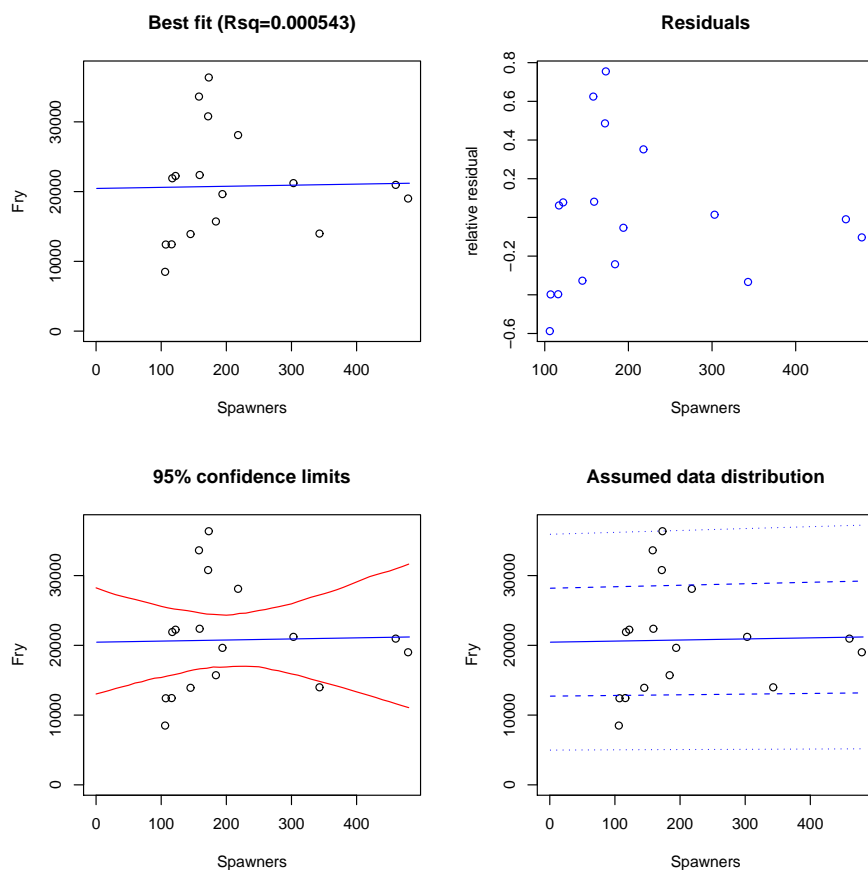


Figure 31: *Bush Ova-Smolt Parameters*. Top – histograms. Bottom – scattergrams.

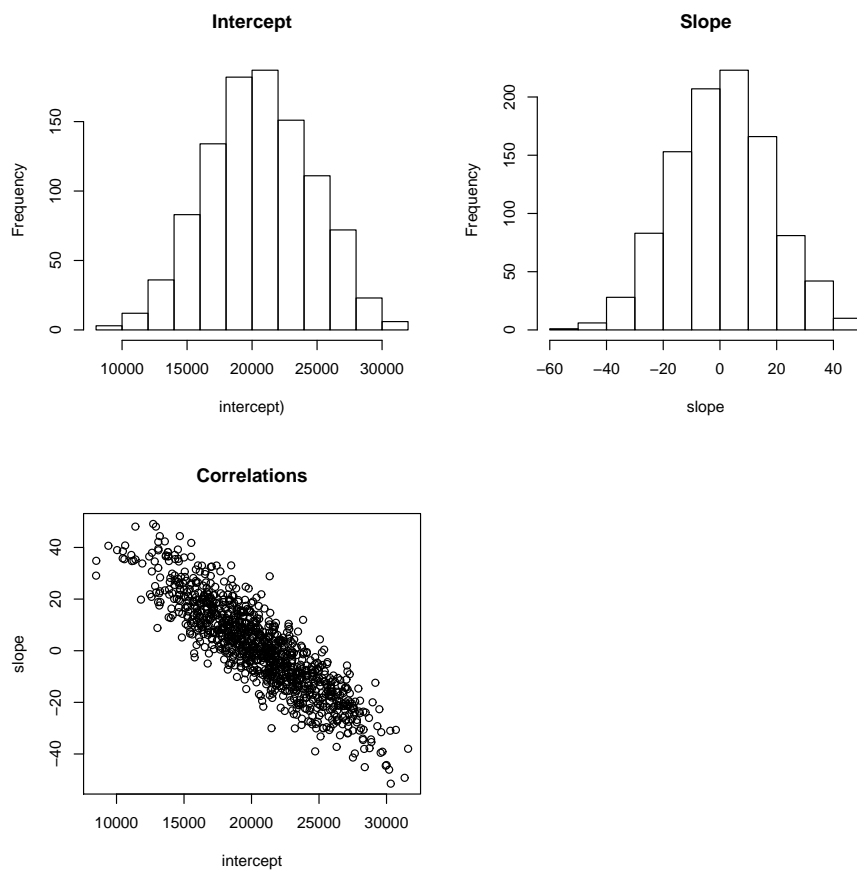
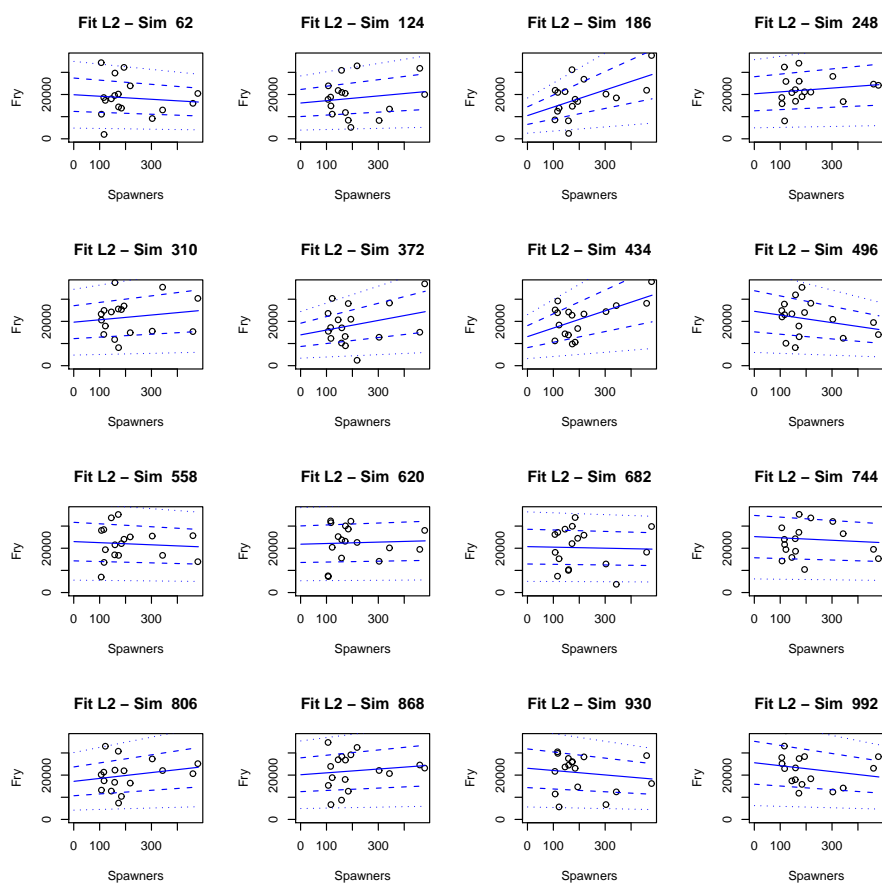


Figure 32: *Bush Ova-Smolt Simulations*

A.8. Straight line: N Esk Spawner \rightarrow Returner

Figure 33: NEsk Spawner-Returner Fits. a) Best fit with data. b) Standardised residuals c) Best fit with 95% confidence limits d) Data with implied mean (solid), one s.d. (dashed) and two s.d. (dotted).

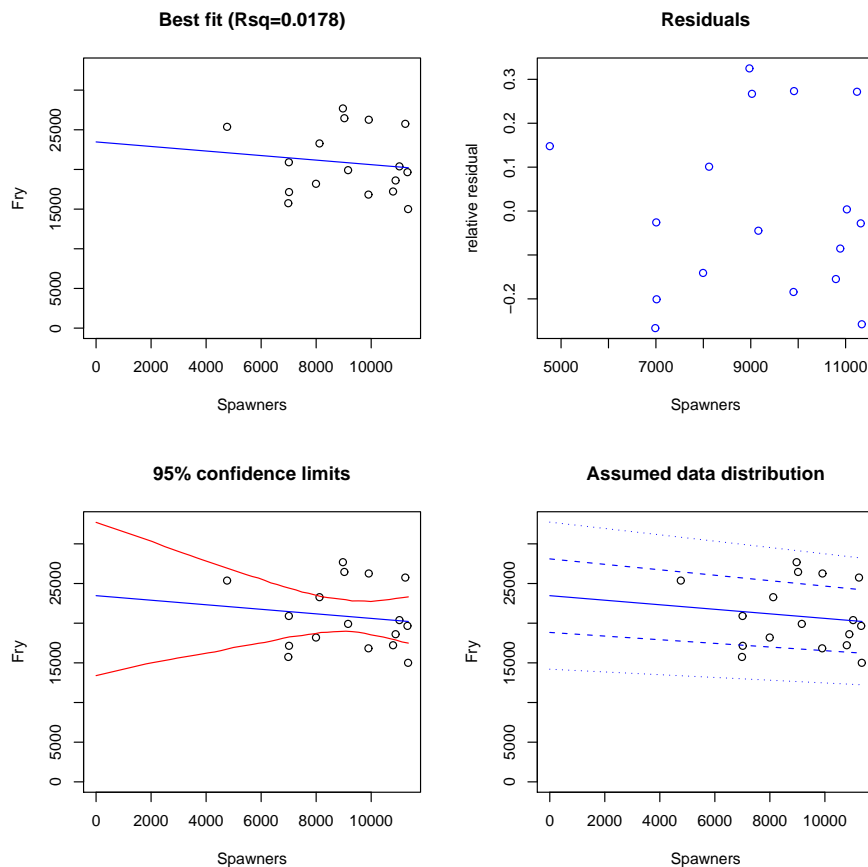


Figure 34: *NEsk Spawner-Returner Parameters. Top – histograms. Bottom – scattergrams.*

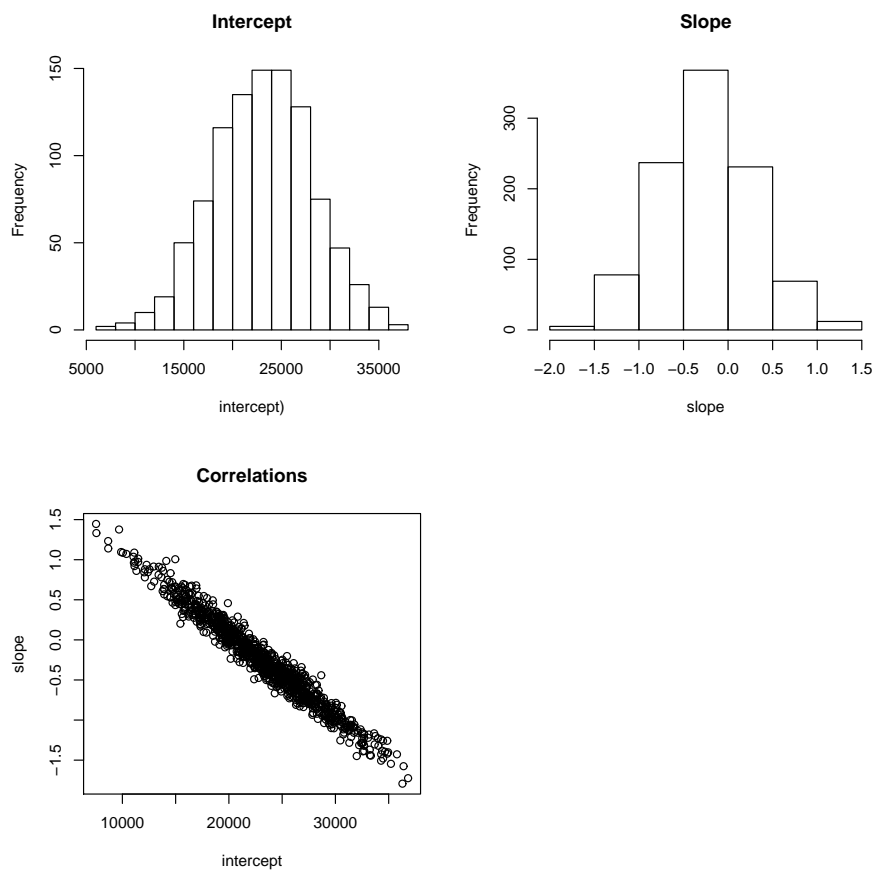
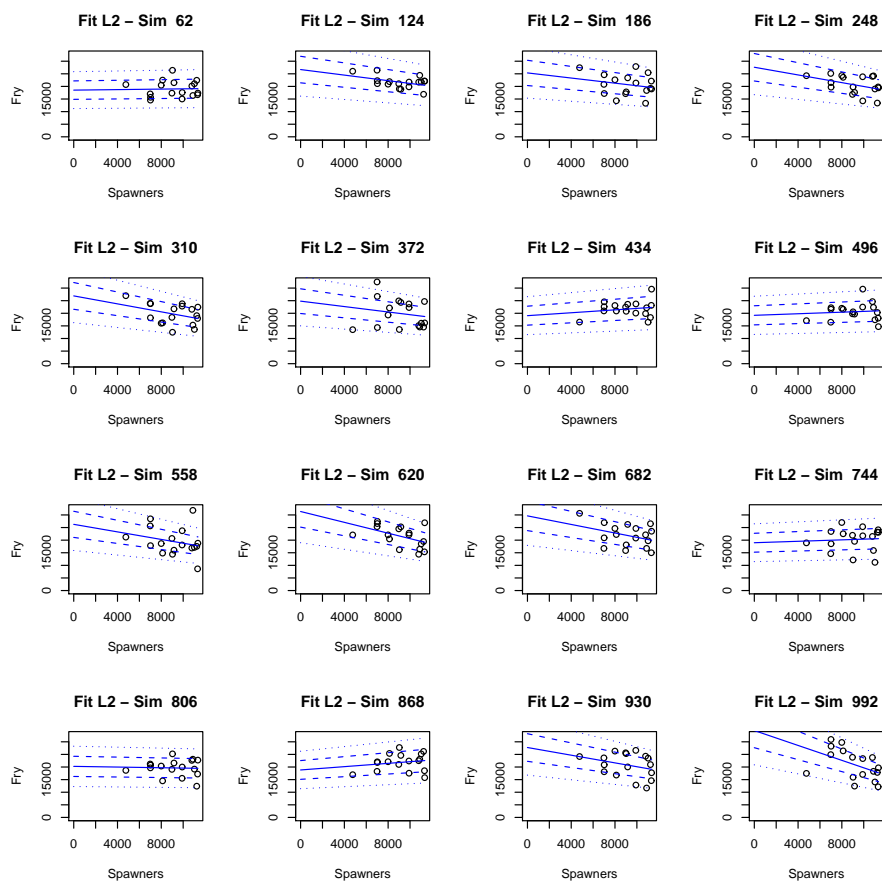


Figure 35: *NEsk Spawner-Returner Simulations*

B. R code

B.1. The generation by generation single deme model

```

%*****
%               R-code to simulate the single deme model
%*****

nextS<-function(S,Rmax=30000,Smax=120,k=1,
                Theta=10,meanP=0.006,cvP=0.1)
{ meanR<-Rmax*(S/Smax)^k*exp(k-k*S/Smax);
  Rnext<-rnbino(1,size=Theta,mu=meanR);
  P<-meanP*(1+rnorm(1,mean=0,sd=cvP))
  Snext<-P*Rnext;
  return(Snext);
}

make.sequence<-function(max.year=1000,
                        init.S=c(65,50,70,100,75),
                        prop.ret=c(0,0,0,0,1,1,0),
                        Rmax=30000,Smax=120,k=1,Theta=10,
                        meanP=0.006,cvP=0.1)
{ prop.ret<-prop.ret/sum(prop.ret);
  sl<-length(prop.ret);
  seq<-vector(mode='double',length=max.year+sl);
  seq[1:length(init.S)]<-init.S;

  for (y in 1:max.year)
    { new<-prop.ret*nextS(seq[y],Rmax,Smax,k,Theta,meanP,cvP);
      seq[(y+1):(y+sl)]<-seq[(y+1):(y+sl)]+new;
    }
  o<-data.frame(year=0:(max.year-1),spawners=seq[1:max.year]);
  return(o);
}

```

B.2. The year by year single deme model

```
nextSC<-function(S,Rmax=4000,Smax=50,Theta=10,meanP=0.02,cvP=0.1)
{ meanF<-ifelse(S>Smax,Rmax,Rmax*S/Smax);
  Rnext<-rnbino(1,size=Theta,mu=meanF);
  P<-meanP*(1+rnorm(1,mean=0,sd=cvP))
  Snext<-P*Rnext;
  return(Snext);
}
```

```
make.sequenceC<-function (max.year=1000,
                          init.S=c(65,50,70,100,75,63,80),
                          prop.ret=c(0,0,0,0,1,1,0),
                          Rmax=4000, Smax=50, sCL=NA, Rho=0.5,
                          Theta=10, meanP=0.04, cvP=0.1)
{ prop.ret<-prop.ret/sum(prop.ret);
  if(!is.na(Rer)){init.S<-init.S/Rer;}
  sl<-length(prop.ret);
  seq<-vector(mode='double',length=max.year+sl);
  cat<-seq;
  seq[1:length(init.S)]<-init.S;

  for (y in 2:max.year)
    { if (is.na(sCL)) {cat[y]<-seq[y]*Rho;}
      else          { allowed<-max(0,seq[y-1]-sCL);
                    cat[y]<-min(seq[y],allowed)
                  }
      seq[y]<-seq[y]-cat[y];
      new<-prop.ret*nextSC(seq[y],Rmax,Smax,Theta,meanP,cvP);
      seq[(y+1):(y+sl)]<-seq[(y+1):(y+sl)]+new;
    }
  o<-data.frame(year=0:(max.year-1),
                spawners=seq[1:max.year],
                catch=cat[1:max.year]);
  return(o);
}
```



```

#####
#                               Fertilise                               #
# Assumes that grilse(cross,multi) mothers produce Eg(Ex,Em) eggs and that #
# the male assemblage which fertilises these eggs contains Mg(Mx,Mm) males of #
# grilse (cross,msw) type. Returns a vector containing the recruitments of #
# females and males of types g,x,m ordered RfG,RfX,RfM,RMg,RMx,RMm. #
# Calculation is deterministic and assumes one locus two allele genetics #
# with random mating in which all functions msw males (x,m) have the same #
# fecundity and grilse males have a reduced fecundity given by the field #
# MaleRelFert in the grilse parameter record #
#####
Fertilise<-function(Eg,Ex,Em,Mg,Mx,Mm,ParG)
{ Tm<-ParG$MaleRelFert*Mg+Mx+Mm;
  if(Tm==0){Pg<-0;Px<-0;Pm<-0}
  else {Pg<-ParG$MaleRelFert*Mg/Tm; Px<-Mx/Tm; Pm<-Mm/Tm;}
  Rg<-Eg*(Pg+Px/2)+Ex*(Pg/2+Px/4);
  Rx<-Ex/2+Eg*(Pm+Px/2)+Em*(Pg+Px/2);
  Rm<-Em*(Pm+Px/2)+Ex*(Pm/2+Px/4);
  return(c(0.5*Rg,0.5*Rx,0.5*Rm,0.5*Rg,0.5*Rx,0.5*Rm));
}

#####
#                               Escapement                               #
# given numbers returning to the river (order Fg..Fm,Mg..Mm) and para records #
# for grilse (ParG) and MSW (ParM), returns a vector (order Fg,Fx,Fm,Mg,Mx,m) #
# of numbers surviving to spawn. If (DetSim) then calculation id deterministic#
# otherwise numbers surviving are assumed to be neg binom with mean=det value #
# and theta=ThetaRiver from appropriate param record #
#####
Escapement<-function(Fg,Fx,Fm,Mg,Mx,Mm,ParG,ParM,DetSim)
{ TVec<-c(ParG$ThetaRiver,ParM$ThetaRiver,ParM$ThetaRiver,
  ParG$ThetaRiver,ParM$ThetaRiver,ParM$ThetaRiver);
  Esc.mean<-c(Fg*ParG$RiverSurvProb, Fx*ParM$RiverSurvProb, Fm*ParM$RiverSurvProb,
  Mg*ParG$RiverSurvProb, Mx*ParM$RiverSurvProb, Mm*ParM$RiverSurvProb);
  if(DetSim) {Esc<-Esc.mean}
  else {Esc<-rnbino(6,mu=Esc.mean,size=TVec)}
  return(Esc)
}

#####
#                               Stock.Rec                               #
# Returns the mean number of surviving recruits (of any sex) produced by fem #
# females in an environment defined by parameter record P which MUST contain #
# fields Rmax,k, and Smax to define a modified Ricker stock-recruit curve #
#####
Stock.Rec<-function(Fem,P)
{Rm<-P$Rmax; k<-P$k; Sm<-P$Smax;
  R<-Rm*(Fem/Sm)^k*exp(k-k*Fem/Sm);
  return(R)
}

```

```

#####
#                               Recruits                               #
# Calculates a stochastic (or deterministic) recruitment appropriate to a #
# deme population {G,X,M} with grilse parameters ParG and msw parameters ParM.#
# G,X and M are total populations (male+female). Egg output is calculated #
# from the base S-R function meanR and variability is negbinom #
# fertilisation is defined by the function 'fertilise' #
# if DetSim=T then calculation is stochastic, otherwise deterministic #
#####
Recruits<-function(Fg,Fx,Fm,Mg,Mx,Mm,ParG,ParM,DetSim)
{Eg.mean<-Stock.Rec(Fg,ParG);
 Emsw.mean<-Stock.Rec(Fx+Fm,ParM);
 if(DetSim)
   { Eg<-Eg.mean;
     Emsw<-Emsw.mean
   }
 else { Eg<-rnbinom(1,mu=Eg.mean,size=ParG$ThetaRec);
       Emsw<-rnbinom(1,mu=Emsw.mean, size=ParM$ThetaRec);
     }
 if(Fx==0){Ex<-0} else {Ex<-Emsw*Fx/(Fx+Fm)};
 if(Fm==0){Em<-0} else {Em<-Emsw*Fm/(Fx+Fm)};
 R<-Fertilise(Eg,Ex,Em,Mg,Mx,Mm,ParG)

 return(R)
}

```

```

#####
#                               make.deme.sequence                               #
#####
make.deme.sequence<-function(MaxYear,ParG,ParM,DetSim=F)
{
# Force return distributions to normalise                                     #
GrRetDistM<-ParG$RetDistM/sum(ParG$RetDistM);
GrRetDistF<-ParG$RetDistF/sum(ParG$RetDistF);
MswRetDistM<-ParM$RetDistM/sum(ParM$RetDistM);
MswRetDistF<-ParM$RetDistF/sum(ParM$RetDistF);

# calculate differential male/female sea-survivals to get correct sex-ratio #
ssFg<-2*ParG$PropFemale*ParG$SeaSurvProb;
ssMg<-2*(1-ParG$PropFemale)*ParG$SeaSurvProb;
ssFm<-2*ParM$PropFemale*ParM$SeaSurvProb;
ssMm<-2*(1-ParM$PropFemale)*ParM$SeaSurvProb;
SeaSurvVec<-c(ssFg,ssFm,ssFm,ssMg,ssMm,ssMm);

# set up and initialise vectors for each population component               #
lg<-length(GrRetDistF); lm<-length(MswRetDistF); maxl<-max(lg,lm);
lini<-max(length(ParG$initGf),length(ParM$initMf),length(ParM$initXf),
           length(ParG$initGm),length(ParM$initMm),length(ParM$initXm));
Fg<-vector('double',length=MaxYear+maxl+1); for (i in 1:length(Fg)){Fg[i]<-0}
Fx<-Fg; Fm<-Fg; Mg<-Fg; Mx<-Fg; Mm<-Fg;
Fg[1:length(ParG$initGf)]<-ParG$initGf;
Fx[1:length(ParM$initXf)]<-ParM$initXf;
Fm[1:length(ParM$initMf)]<-ParM$initMf;
Mg[1:length(ParG$initGm)]<-ParG$initGm;
Mx[1:length(ParM$initXm)]<-ParM$initXm;
Mm[1:length(ParM$initMm)]<-ParM$initMm;

# run system forward for years 1->MaxYear
for(y in 1:MaxYear)
{
# If y>length of initial conditions assume number of fish curently in
# year y cells is number returning to coast.Calculate number who survive to
# spawn and update year y cells to spawning population. Else force cell
# back to initial state.
if (y>lini)
{ esc<-Escapement(Fg[y],Fx[y],Fm[y],Mg[y],Mx[y],Mm[y],ParG,ParM,DetSim);
  Fg[y]<-esc[1]; Fx[y]<-esc[2]; Fm[y]<-esc[3];
  Mg[y]<-esc[4]; Mx[y]<-esc[5]; Mm[y]<-esc[6];
}
else
{ Fg[y]<-ParG$initGf[y]; Fx[y]<-ParM$initXf[y]; Fm[y]<-ParM$initMf[y];
  Mg[y]<-ParG$initGm[y]; Mx[y]<-ParM$initXm[y]; Mm[y]<-ParM$initMm[y];
}

# Calculate number of recruits from spawning population in year y
RecVec<-Recruits(Fg[y],Fx[y],Fm[y],Mg[y],Mx[y],Mm[y],ParG,ParM,DetSim);

# Calculate mean number of survivors from these recruits and distribute
# each group across the years in which it may return.
RetVec<-RecVec*SeaSurvVec;
RetFg.mean<-RetVec[1]*GrRetDistF; RetMg.mean<-RetVec[4]*GrRetDistM;
}
}

```

```

RetFx.mean<-RetVec[2]*MswRetDistF; RetMx.mean<-RetVec[5]*MswRetDistM;
RetFm.mean<-RetVec[3]*MswRetDistF; RetMm.mean<-RetVec[6]*MswRetDistM;

# Calculate the actual number of survivors for each sex, genotype and
# year of return
if(DetSim) {RetFg<-RetFg.mean; RetFx<-RetFx.mean; RetFm<-RetFm.mean
           RetMg<-RetMg.mean; RetMx<-RetMx.mean; RetMm<-RetMm.mean}
  else     {RetFg<-rnbinom(lg,mu=RetFg.mean,size=ParG$ThetaSea);
           RetFm<-rnbinom(lm,mu=RetFm.mean,size=ParM$ThetaSea);
           RetFx<-rnbinom(lm,mu=RetFx.mean,size=ParM$ThetaSea);
           RetMg<-rnbinom(lg,mu=RetMg.mean,size=ParG$ThetaSea);
           RetMm<-rnbinom(lm,mu=RetMm.mean,size=ParM$ThetaSea);
           RetMx<-rnbinom(lm,mu=RetMx.mean,size=ParM$ThetaSea);}

# Add survivors for each sex, year, genotype and year of return to
# that years total
Fg[(y+1):(y+lg)]<-Fg[(y+1):(y+lg)]+RetFg;
Fx[(y+1):(y+lm)]<-Fx[(y+1):(y+lm)]+RetFx;
Fm[(y+1):(y+lm)]<-Fm[(y+1):(y+lm)]+RetFm;
Mg[(y+1):(y+lg)]<-Mg[(y+1):(y+lg)]+RetMg;
Mx[(y+1):(y+lm)]<-Mx[(y+1):(y+lm)]+RetMx;
Mm[(y+1):(y+lm)]<-Mm[(y+1):(y+lm)]+RetMm;
}

# Load population component vectors into a dataframe and return #
o<-data.frame(year=1:MaxYear,
              Fg=Fg[1:MaxYear],Fx=Fx[1:MaxYear],Fm=Fm[1:MaxYear],
              Mg=Mg[1:MaxYear],Mx=Mx[1:MaxYear],Mm=Mm[1:MaxYear],
              Fgrilse=Fg[1:MaxYear], Fmsw=Fm[1:MaxYear]+Fx[1:MaxYear],
              Mgrilse=Mg[1:MaxYear], Mmsw=Mm[1:MaxYear]+Mx[1:MaxYear])
return(o)
}

#####
#                               plot.deme.sequence                               #
# Uses make.deme.sequence to creat a run MaxYears long controlled by grilse #
# pars Gp and MSW pars Mp. if DetSim then simulation is deterministic o/w #
# stochastic. The first TransLen years are discarded and the rest plotted #
#####
plot.deme.sequence<-function(MaxYear=1500,TransLen=500,
                             Gp=Girnock.70.80.Grilse, Mp=Girnock.70.80.MSW,
                             DetSim=F, plotfile='none')
{ if (plotfile=='none'){x11();}
  else {postscript(plotfile,horizontal=F,paper='special',width=8,height=8)}
  if(TransLen>MaxYear){TransLen<-1};
  WinL<-TransLen+round((MaxYear-TransLen)/2)-25; if(WinL<1){WinL<-1};
  WinR<-TransLen+round((MaxYear - TransLen)/2)+25;
  if(WinR>(MaxYear)){WinR<-(MaxYear)};
  s<-make.deme.sequence(MaxYear,Gp,Mp,DetSim);
  sc<-s[TransLen:MaxYear,];
  par(mfrow=c(3,2),cex.axis=1.5,cex.lab=1.5);
}

```

```

maxy<-max(sc$Fgrilse+sc$Mgrilse,sc$Fmsw+sc$Mmsw);
GG<-sc$Fg+sc$Mg;
mgg<-mean(GG); sgg<-sd(GG);
pt<-paste('GG: mean=',round(mgg,1),' cv=',round(sgg/mgg,3),sep='');
plot(sc$year,GG,type='l',main=pt,xlab='year',ylab='number');

GM<-sc$Fx+sc$Mx;
mgm<-mean(GM); sgm<-sd(GM);
pt<-paste('GM: mean=',round(mgm,1),' cv=',round(sgm/mgm,3),sep='');
plot(sc$year,GM,type='l',main=pt,xlab='year',ylab='number');

if(DetSim)
{ MM<-sc$Fm+sc$Mm;
  mmm<-mean(MM); smm<-sd(MM);
  pt<-paste('MM: mean=',round(mmm,1),' cv=',round(smm/mmm,3),sep='');
  plot(sc$year,MM,type='l',main=pt,xlab='year',ylab='number');
}

grilse<-sc$Fgrilse+sc$Mgrilse; msw<-sc$Fmsw+sc$Mmsw;
mg<-mean(grilse); cvg<-sd(grilse)/mg;
mm<-mean(msw); cvm<-sd(msw)/mm;
pt<-paste('MSW(Gr) mean=',round(mm),'(',round(mg),
          ') cv=',round(cvm,2),'(',round(cvg,2),')',sep='');
plot(sc$year,grilse,type='l',ylim=c(0,maxy),
      col='red',main=pt,xlab='year',ylab='number');
lines(sc$year,msw,col='blue')

mxy<-2+max( sc$Fgrilse,sc$Mgrilse,sc$Fmsw,sc$Mmsw)
plot(sc$year,sc$Fgrilse,main='Fluctuations by sex and sea-age',xlab='year',
      ylab='number',type='l',xlim=c(WinL,WinR),ylim=c(0,mxy),col='red')
lines(sc$year,sc$Mgrilse,col='red',lty=3);
lines(sc$year,sc$Fmsw,col='blue');
lines(sc$year,sc$Mmsw,col='blue',lty=3);

if(DetSim)
{ plot(sc$year,grilse/(grilse+msw),type='l',ylim=c(0,1),col='black',
      xlab='year',ylab='Proportion',main='Proportions')
  lines(sc$year,sc$Fg/(sc$Fg+sc$Mg),col='red');
  lines(sc$year,(sc$Fx+sc$Fm)/(sc$Mx+sc$Mm+sc$Fx+sc$Fm),col='blue');
}
else
{ a<-acf(msw,plot=F);
  plot(a,xlim=c(0,20),xlab='lag(year)',ylab='correlation',
       main='ACF(salmon)');

  c<-ccf(grilse,msw,plot=F);
  plot(c,xlim=c(-10,10),xlab='lag(year)',ylab='correlation',
       main='CCF(grilse,salmon)');
}

if(plotfile!='none'){dev.off()}
}

```

```

#####
#                               make.step.change                               #
# Spins up the system deterministically for InitY years using params Gpi,Mpi   #
# Makes one deterministic and Nproj stochastic projections over MaxProjYear  #
# years. Returns list containing the deterministic projection in the standard  #
# make.deme.sequence format and returns the states of all the stochastic     #
# projections at 1/4, 1/2, 3/4 and 4/4 of the designated projection period    #
#####
make.step.change<-function(Gpi=Girnock.70.80.Grilse, Mpi=Girnock.70.80.MSW,
                           Gpf=Girnock.90.00.Grilse, Mpf=Girnock.90.00.MSW,
                           InitY=500,MaxProjYear=50,Nproj=300)
{ si<-make.deme.sequence(MaxYear=InitY,ParG=Gpi,ParM=Mpi,DetSim=T);
  Gpf$initGf<-si$Fg[(InitY-length(Gpf$initGf)):InitY];
  Mpf$initXf<-si$Fx[(InitY-length(Mpf$initXf)):InitY];
  Mpf$initMf<-si$Fm[(InitY-length(Mpf$initMf)):InitY];
  Gpf$initGm<-si$Mg[(InitY-length(Gpf$initGm)):InitY];
  Mpf$initXm<-si$Mx[(InitY-length(Mpf$initXm)):InitY];
  Mpf$initMm<-si$Mm[(InitY-length(Mpf$initMm)):InitY];

  det<-make.deme.sequence(MaxYear=MaxProjYear,ParG=Gpf,ParM=Mpf,DetSim=T);
  result<-list(final=data.frame(proj=1:Nproj,Fg=NA,Fx=NA,Fm=NA,Mg=NA,Mx=NA,Mm=NA),
               half=data.frame(proj=1:Nproj,Fg=NA,Fx=NA,Fm=NA,Mg=NA,Mx=NA,Mm=NA),
               Tq=data.frame(proj=1:Nproj,Fg=NA,Fx=NA,Fm=NA,Mg=NA,Mx=NA,Mm=NA),
               Q=data.frame(proj=1:Nproj,Fg=NA,Fx=NA,Fm=NA,Mg=NA,Mx=NA,Mm=NA)
               )
  for(proj in 1:Nproj)
    {sp<-make.deme.sequence(MaxYear=MaxProjYear,ParG=Gpf,ParM=Mpf,DetSim=F);
      result$final[proj,2:7]<-sp[MaxProjYear,2:7];
      result$half[proj,2:7]<-sp[round(MaxProjYear/2),2:7];
      result$Tq[proj,2:7]<-sp[round(3*MaxProjYear/4),2:7];
      result$Q[proj,2:7]<-sp[round(MaxProjYear/4),2:7];
    }
  return(list(det=det,prob=result));
}

```

```

#####
#                               plot.step.change                               #
# Uses make.step.change to create a projection for a change from Gpi,Mpi to   #
# Gpf,Mpf. Plots the deterministic projectins and the probability distributions #
# for half and full-time projections                                         #
#####
plot.step.change<-function(Gpi=Girnock.70.80.Grilse, Mpi=Girnock.70.80.MSW,
                           Gpf=Girnock.90.00.Grilse, Mpf=Girnock.90.00.MSW,
                           InitY=500,MaxProjYear=100,Nproj=1000,plotfile='none')
{
  result<-make.step.change(Gpi,Mpi,Gpf,Mpf,InitY,MaxProjYear,Nproj);

  if(plotfile=='none'){x11()}
  else {postscript(plotfile,horizontal=F,paper='special',width=8,height=8)}
  par(mfrow=c(3,2));
  det<-result$det;
  dg<-det$Fgrilse+det$Mgrilse; maxy<-max(dg);
  plot(det$year,dg, main='Deterministic: Grilse',
        xlab='year',ylab='Number',ylim=c(0,maxy),type='l');
  lines(det$year,det$Fgrilse,col='red');
  lines(det$year,det$Mgrilse,col='red',lty=2);

  dmsw<-det$Mmsw+det$Fmsw; maxy<-max(dmsw);
  plot(det$year,dmsw,main='Deterministic: MSW',
        xlab='year',ylab='Number',ylim=c(0,maxy),type='l');
  lines(det$year,det$Fmsw,col='blue');
  lines(det$year,det$Mmsw,col='blue',lty=2);

  pf<-result$prob$half; pgf<-pf$Fg+pf$Mg; py<-round(MaxProjYear/2);
  mc<-paste(py,' Years - Grilse Probability',sep='');
  hist(pgf,freq=F,xlab='total grilse', main=mc);

  pmf<-pf$Fx+pf$Mx+pf$Fm+pf$Mm;
  mc<-paste(py,' Years - Grilse Probability',sep='');
  hist(pmf,freq=F,xlab='total msw', main=mc);

  pf<-result$prob$final; pgf<-pf$Fg+pf$Mg;
  mc<-paste(MaxProjYear,' Years - Grilse Probability',sep='');
  hist(pgf,freq=F,xlab='total grilse', main=mc);

  pmf<-pf$Fx+pf$Mx+pf$Fm+pf$Mm;
  mc<-paste(MaxProjYear,' Years - MSW Probability',sep='');
  hist(pmf,freq=F,xlab='total msw', main=mc);
  if(plotfile!='none'){dev.off()}
}

```